Available online at www.sciencedirect.com
SCIENCE DIRECT®
International Journal of Mass Spectrometry 237 (2004) 75–105
International Journal of Mass Spectrometry
www.elsevier.com/locate/ijms

Review

On the spin-forbiddeness of gas-phase ion–molecule reactions: a fruitful intersection of experimental and computational studies

Helmut Schwarz*

Institut für Chemie der Technischen, Universität Berlin, Straße des 17. Juni 135, D-10623 Berlin, Germany

Received 23 April 2004; accepted 10 June 2004

Dedicated to Alan G. Marshall on the occasion of his 60th birthday and in recognition of his fundamental contributions to mass spectrometry.

Abstract

The effects of spin changes on the efficiencies and product distributions of gas-phase ion–molecule reactions are analyzed, and the examples discussed include metal- as well as non-metal containing systems, with some emphasis on various types of bond activation by 'naked' transition-metal cations and structurally simple cationic transition-metal oxides. Whenever possible, comparison of the experimental findings with computational studies will be made, and the agreement is generally good if not excellent.

Keywords: Bond activation; Computational chemistry; Ion–molecule reactions; Mass spectrometry; Molecular orbital symmetry; Spin–orbit coupling; Oxidation chemistry; Potential energy surfaces; Transition-metal chemistry

1. Introduction

The mental representation of chemical reactions relies on the paradigm of the potential energy surface (PES): the reactive systems move from the reactant minimum of the PES through transition states and intermediates to the product minimum. Reactions, which involve a change in total electronic spin, appear to violate this paradigm, since they must necessarily occur on two or more PESs. While spin-nonconserving reactions are often referred to as 'forbidden', it is in fact more appropriate to ascribe to them a certain degree of spin-forbiddeness which is controlled by the magnitude of the spin–orbit coupling (SOC) term of the system's Hamiltonian operator. There is actually a continuum of 'forbiddeness' being largest when the affected electrons are localized on light atoms, such as first row elements and much less so for the heavier 4f, 5d and 5f elements. Transition metals from the 3d block, the gas-phase ion chemistry of which will form the central part of this review, constitute intermediate cases. Clearly, in the limit of very strong spin–orbit coupling between the different states involved, such a reaction occurs on a single adiabatic potential energy surface whose spin character changes smoothly in the course of the chemical transformation. When SOC is weaker, the reaction will behave in a non-adiabatic way, and several electronic states determine the outcome. While many 'spin-forbidden' processes are well-recognized, encompassing, e.g., predissociation in spectroscopy [1a,b], the role of spin-inversion in photochemistry [1c–f], and spin-crossover in transition-metal chemistry [2], just to mention a few, misconceptions about the role of spin in chemical reactivity are common despite excellent review articles highlighting the problem, presenting convincing examples and proposing computational means on how to clarify the situation [3].

Nevertheless, it is true that often the Wigner–Witmer spin conservation rule accounts for the observed low probability of a number of *exothermic* ion–molecule reactions in which electronic spin angular momentum is not conserved. For example, the spin-forbidden reactions (1) and (2) proceed with rates at least 10^2 times slower than similar but spin-allowed reactions [4].

$$CO_2{}^+(^2\Pi) + N(^4S) \rightarrow NO^+(^1\Sigma) + CO(^1\Sigma) \quad (1)$$

* Tel.: +49 30314 23483; fax: +49 30314 21102.
E-mail address: Helmut.Schwarz@mail.chem.tu-berlin.de (H. Schwarz).

1387-3806/$ – see front matter © 2004 Elsevier B.V. All rights reserved.
doi:10.1016/j.ijms.2004.06.006

$$NO^+(^1\Sigma) + O_3(^1A) \rightarrow NO_2{}^+(^1\Sigma) + O_2(^3\Sigma) \quad (2)$$

Exceptions can arise in the presence of strong coupling of the electronic spin and orbital angular momentum as is apparently the case for the spin-forbidden reaction (3) which occurs with efficiency close to the collision rate [5a,b]. For interesting spin–orbit effects in the O^+/N_2 system, see Ref. [5c].

$$O^+(^4S) + CO_2(^1\Sigma) \rightarrow O_2{}^+(^2\Pi) + CO(^1\Sigma) \quad (3)$$

In this Review examples of *thermal* gas-phase reactions of ionic species from three areas will be discussed, common to which is the central role of an apparent electronic spin-violation. We shall begin with a brief discussion of both bimolecular and unimolecular processes of systems, which are comprised of only main-group elements. This section will be followed by a thorough presentation of the intriguing role 'naked' transition-metal cations play in the activation of various X−H bonds (X = H, C, Si, O, N, etc.). The chapter on bond activation by metal ion–molecule reactions is preceded by mentioning a few examples of metal–ligand association and ligand-exchange processes, the efficiency of which is also affected by spin–orbit coupling factors. Finally, some aspects of the rich gas-phase ion chemistry of cationic transition-metal oxides will be highlighted, and for a few systems the relevance of this seemingly esoteric chemistry and its bearing on selected fundamental chemical transformations, e.g., C−H bond oxygenation under homogeneous, heterogeneous and enzymatic conditions, will be outlined. Whenever possible, experimental and theoretical findings will be compared. Most of the experiments employed advanced, if not state-of-the-art, mass spectrometric methods that allow the generation of mass-selected, electronic ground state species and to explore their chemistry under well-defined unimolecular and/or (mostly) single-collision conditions. Rather than giving a description of the various experimental techniques, the interested reader is referred to the original references. Similarly, no computational details are presented on how to locate the minimum energy crossing points (MECPs) between different states, an aspect which is absolutely crucial for a semi-quantitative description of reactions in which different spin surfaces are involved. For leading references and a superb discussion of the underlying principles, concepts and technical problems, consultation of references [1a,b,3h,j,k,1,6] is recommended.

2. Unimolecular and bimolecular spin-forbidden gas-phase processes of metal-free systems

Proton transfers between anions and neutral acids are among the most ubiquitous reactions in chemistry, and for simple, i.e., non-resonance stabilized, anions exoergic proton transfer in the gas phase generally proceeds with nearly collision rate [7]. However, spin-conservation aspects clearly matter as has been demonstrated in a series of elegant studies. Tanaka et al. [8] have examined and identified in detail such spin-forbidden reactions:

$$C^-(^4S) + XH(\text{singlet}) \rightarrow X^-(\text{singlet}) + CH(^2\Pi) \quad (4)$$

However, the violation of the spin conservation rule can be avoided for the more exothermic members of this series by the spin-allowed production of CH in the low lying $^4\Sigma$ excited state:

$$C^-(^4S) + XH(\text{singlet}) \rightarrow X^-(\text{singlet}) + CH(^4\Sigma) \quad (5)$$

As the term energy of $CH(^4\Sigma)$ is around 17 kcal/mol [9], reactions with an exothermicity ($\Delta_r H$) less than 17 kcal/mol were expected to show a low reaction probability and that with $\Delta_r H$ larger than 17 kcal/mol should exhibit an increase in reaction probability. These expectations were born out in flowing afterglow experiments, for the 'weak' acids CH_3COCH_3 and SiH_4 possess reaction efficiencies of only 1.9 and 3.6%; in contrast, the probability of proton transfer was enhanced by more than a factor of 10 for the more exothermic reactions of C^- with XH = H_2S, HCN and HCl. This enhancement was attributed to the spin-allowed production of excited $CH(^4\Sigma)$ according to reaction (5).

In the same vein, the different rates with which triplet NO^- is protonated, depending on the acidity of the proton source, can be accounted for by spin considerations. The weakly exothermic reaction of NO^- with CH_3NO_2 ($\Delta_r H$ = −6 kcal/mol) is not observed under thermal conditions [10a] and this absence of reactivity is ascribed to the spin-forbiddeness to produce ground-state HNO in its singlet state. In contrast, reaction of NO^- with HCl is very rapid [10b] (For a detailed study of various aspects of spin-forbidden deprotonation of *aqueous* HNO), and it is likely that in a spin-allowed process due to the large exothermicity ($\Delta_r H$ = −35 kcal/mol) $^3NO^-$ is converted to excited ^{3}HNO; as ^{3}HNO is only 18 kcal/mol less stable than ^{1}HNO it is energetically accessible in the reaction with HCl but not with CH_3NO_2 [10c].

Further, while the details of the spin dynamics are not yet fully resolved [11], there is no doubt that a spin change is involved in the proton transfer reaction (6), which is quite efficient for this slightly exothermic ($\Delta_r H$ = −8 kcal/mol) process despite the modest spin–orbit coupling in isolated NO. The authors believe that the lifetime of the intermediate $[FHNO]^-$ complex is long enough to allow for SOC, and the energy required to reach the curve crossing region in the proton transfer between the encounter complexes $F^-\cdot{}^1$HNO and $FH\cdot{}^3NO^-$ is low.

$$F^- + {}^1HNO \rightleftharpoons [FHNO]^- \rightleftharpoons HF + {}^3NO^- \quad (6)$$

Another remarkable gas-phase example of a conjugate *organic* acid–base pair with different spin multiplicities, a situation, which is exceedingly rare [12], was described by Squires and co-workers [13]. The proton affinity (PA) of (3-oxyphenyl)methylene anion (**1**) was experimentally determined to PA = 343.0 kcal/mol. This number is in excellent agreement with the value predicted by extensive calculations

for *oxygen*-protonation of *singlet* **1** to give the *triplet* of (3-hydroxyphenyl)methylene (**2**), but is significantly different from the values calculated for any other conceivable spin-state conversions of **1** and **2**. Consequently, in this system the 'spin barrier' for adiabatic proton transfer to ion **1**, Eq. (7), cannot be very large and the intersystem crossing must be fast on the time scale of the intermediate's lifetime.

$$\ddot{HCC}_6H_4O^-(^1\mathbf{1}) + HX(\text{singlet}) \rightarrow \ddot{HCC}_6H_4OH(^3\mathbf{2}) + X^-(\text{singlet}) \quad (7)$$

The kinetic energy dependence of the cross-sections for the reactions of ground and excited state atomic sulfur ions with H_2, Eq. (8), and its isotopic variants HD and D_2, has been studied experimentally and computationally [14].

$$S^+ + H_2 \rightarrow SH^+ + H \quad (8)$$

For the ^4S ground state of S^+, the cross-section exhibits two distinct features: The low-energy endothermic feature has a threshold consistent with the thermodynamic limit of reaction (8), and based on the isotope distribution in the reaction of S^+ with HD, a statistically behaved intermediate is implied. This pathway is attributed to a spin-forbidden transition between the reactant $^4A''(A_2)$ potential energy surface and a $^2A''(B_1)$ surface, which correlates with the electronic ground state of the H_2S^+ intermediate. As expected for a formally spin-forbidden process, the efficiency of this low-energy pathway is rather small as found in the guided ion-beam experiments.

Spin aspects can also matter in *unimolecular* dissociations, and the discussion of a few cases may suffice. A typical example which has formed the subject of numerous studies [15] is the unimolecular decomposition of triplet methoxy cation ($^3CH_3O^+$) to form H_2 and formyl cation (HCO^+), both singlet species. The process can occur in a stepwise manner, Eq. (9), i.e., first hydrogen shift, concurrent with or followed by a spin change, to form singlet hydroxymethyl cation ($^1CH_2OH^+$), then the well-documented [1.2]-elimination [16] to yield $^1HCO^+$ and H_2. While this two-step reaction was favoured for quite a while, a *concerted* ('direct') pathway, Eq. (10), involving simultaneous spin change and [1.1]-elimination from $^3CH_3O^+$ had been suggested [17], but not established.

$$^3CH_3O^+ \rightarrow {}^1CH_2OH^+ \rightarrow {}^1HCO^+ + H_2 \quad (9)$$

$$^3CH_3O^+ \rightarrow {}^1HCO^+ + H_2 \quad (10)$$

However, a combination of detailed isotope effect analysis, extensive electronic structure calculations of the potential energy surfaces and the application of non-adiabatic RRKM theory [15,18] has clarified the situation in favour of Eq. (10). As can be seen in Fig. 1, the direct pathway (Eq. (10)) involves migration of two hydrogen atoms towards each other and away from carbon, to lead, after spin inversion at the minimum energy crossing point MECP1, directly to the product channel. The indirect route (Eq. (9)) involves migration of one hydrogen atom away from carbon and towards oxygen. After spin change at MECP2 this leads to $^1CH_2OH^+$, which in turn can dissociate adiabatically through a cyclic transition state to give HCO^+ and H_2. What is important is that (i) the spin–orbit coupling between the PESs is of the same magnitude at both crossing points [15,19] and (ii) at all levels of theory employed [18] MECP1 is located below MECP2, thus resulting in higher rate coefficients for the direct pathway, Eq. (10) [18].

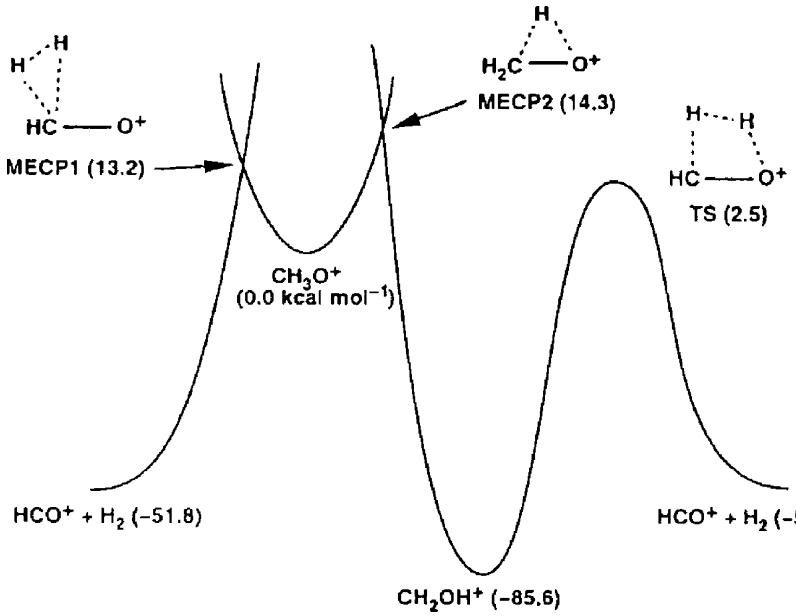

Fig. 1. Schematic singlet and triplet potential energy curves of the $[CH_3O]^+$ system, calculated at the CCSD(T)/CC–pVTZ(–d)//B3LYP/6–311+G(d,p) level of theory. Relative energies in kcal/mol. See references [15,18] for further details. Reproduced from *Phys. Chem. Chem. Phys*. 1 (1999) 5555.

In many respects closely related to the CH_3O^+ system is the gas-phase chemistry of the thiomethoxy cation CH_3S^+, for which the prevailing unimolecular dissociation corresponds to the spin-forbidden dehydrogenation:

$$CH_3S^+(^3A_1) \rightarrow HCS^+(^1\Sigma^+) + H_2(^1\Sigma_g^+) \quad (11)$$

Mechanistic insight was recently provided by two in-depth theoretical studies [20] of the potential energy surface and a consideration of various dynamical aspects with regard to reaction (11). It turned out, that for the dehydrogenation of metastable CH_3S^+ two distinct spin-forbidden paths exist, which are mechanistically comparable to the ones characterized for the CH_3O^+ system; however, in contrast to the latter, depending on the degree of ro-vibrational excitation of CH_3S^+ both spin-forbidden reactions, i.e., the 'direct' concerted [1.1]-elimination and the 'stepwise' process compete with each other. Not unexpectedly, the spin–orbit coupling elements of the MECPs are larger for CH_3S^+ than for CH_3O^+, i.e., 221 and 256 cm^{-1} versus 50 and 56 cm^{-1} for MECP1 and MECP2, respectively.

Some of the controversies related to the existence of a long-lived triplet state of $CH_3CH_2S^+$ were resolved recently in a combined experimental/theoretical study [21]. It was found that all exothermic or thermoneutral unimolecular isomerizations or fragmentations of $C_2H_5S^+$ were hampered by spin barriers imposed by the spin-forbiddeness of the various triplet → singlet conversions of the $C_2H_5S^+$ potential energy surfaces, and for triplet $CH_3CH_2S^+$ ions with less than 10 kcal/mol of internal energy the cation should be long-lived as inferred from experiments [21,22].

The unimolecular gas-phase reactions of the protonated isoelectronic molecules of hydrazine (NH_2NH_2), hydroxylamine (NH_2OH), and hydrogen peroxide (HOOH) have been studied experimentally and computationally [23], and those dissociation reactions in which crossovers from the singlet to the triplet electronic states take place are summarized in Eqs. (12)–(14).

$$^1NH_2NH_3^+ \rightarrow {}^1NH_4^+ + {}^3NH \quad (12)$$

$$^1HONH_3^+ \rightarrow {}^1OH_3^+ + {}^3NH \quad (13)$$

$$^1HOOH_2^+ \rightarrow {}^1OH_3^+ + {}^3O \quad (14)$$

For all three reactions not only the lowest energy pathways were calculated, more importantly, the MECPs at which the crossing from the singlet to the triplet surfaces en route to product formation occurs were located and the SOC terms determined; the latter are in the range of 57–73 cm^{-1} which is typical for systems involving first-row elements [1,24]. Common to reactions (12) and (14) is that the crossover from the singlet to the triplet surfaces *precedes* the isomerization to the weakly interacting ionic complexes (Eq. (15)), whereas for the unsymmetrical precursor $^1HONH_3^+$ the spin flip singlet → triplet takes place only after the first hydrogen migration (Eq. (16)).

$$^1HXXH_2^+ \xrightarrow[(2)\sim H]{(1)\,S\rightarrow T} {}^3X\cdots{}^1XH_3 \rightarrow {}^3X + {}^1XH_3^+ \quad (X = NH,\ O) \quad (15)$$

$$^1HONH_3^+ \xrightarrow{(1)\sim H} {}^1H_2ONH_2^+ \xrightarrow[(3)\sim H]{(2)\,S\rightarrow T} {}^1H_3O^+\cdots{}^3NH \rightarrow {}^1H_3O^+ + {}^3NH \quad (16)$$

3. Bond activation by atomic transition-metal cations

3.1. The initial phase: metal ligation

Activation of a bond A–B by a bare transition-metal ion M^+, Eq. (17), is often preceded by oxidative addition [25] which itself follows the formation of an encounter complex. As will be outlined in Chapters 3.2 and 3.3, the combined effects of electronic and kinetic energy, spin, electron configuration and spin–orbit coupling are responsible for the observed variations of rate coefficients, branching ratios, and kinetic isotope effects, and as stated by Weisshaar [3d], for these (and related) bond activation processes by M^+ "each electronic state is potentially a different chemical".

$$M^+ + A{-}B \longrightarrow [M^+(A{-}B)]^* \longrightarrow A{-}M^+{-}B \longrightarrow \begin{cases} MA^+ + B \\ MB^+ + A \end{cases} \quad (17)$$

Ligation of M^+ constitutes the very first step in the bond activation of AB, and therefore it is legitimate to look into the role the electronic structure of M^+ plays at this early stage of Eq. (17)—or to put things in a more general context: To which extent are the energetics and kinetics of (sequential) ion ligation affected by the intrinsic electronic properties of M^+?

While detailed theoretical calculations [26] indicate that the transition-metal ion bonds to ligands as different as H_2O and CO are primarily electrostatic, a comparison of the bond dissociation energies of Co^+ and Fe^+ with various ligands L reveals one trend immediately: the $Co^+{-}L$ bonds are invariably stronger than the analogous $Fe^+{-}L$ bonds [17]. This difference is a direct consequence of the different ground-state configurations of Co^+ and Fe^+, with Co^+ having a $3d^8(^3F)$ and Fe^+ a $4s^13d^6(^6D)$ configuration. Because the 4s orbital is larger than the 3d one, the difference in 4s orbital occupancy

causes a smaller metal–ligand repulsion for Co^+ than for Fe^+, and the ligand can approach the Co^+ metal core more closely, thus resulting in a stronger bond. Promotion to the strongly bonding $3d^7(^4F)$ configuration would remove this problem, but it requires energy of ca. 7 kcal/mol; so in either case, ligands bind less strongly to naked Fe^+ than to bare Co^+.

Other electronic as well as spin effects come into play for the sequential ligations of some of the transition-metal cations. For example, several laboratories reported [27,28] that the *second* H_2O ligand is bound more strongly to most of the first-row transition-metal cations than the first one, and a convincing explanation to these counter-intuitive observations was provided by ab initio calculations for all of the first-row transition-metal complexes $M(H_2O)_n^+$ (n = 1 and 2) [26a]. According to these computational studies, the bonding for the *first* water molecule is primarily electrostatic because such a bond will balance the competition of attractive ion-induced dipole interaction and the electron–electron repulsion of M^+ and the ligand. For one H_2O molecule bound to M^+, the metal ion can minimize the repulsion in two ways: 4s3d or 4s4p hybridization and 4s → 3d promotion. The relative importance of these two options depends on the energy difference between the low-lying $3d^n$ and $4s3d^{n-1}$ states of M^+. For the particular case of $Fe(H_2O)_n^+$ (n = 0–2) the ground state of $Fe(H_2O)^+$ is $^6A_1$ arising from the $^6D(4s3d^6)$ ground state of Fe^+. For a single H_2O ligand, promotion of the cation to the $^4F(3d^7)$ state does not increase the bonding to an extent necessary to compensate sufficiently for the promotion energy; actually, the $^4A_1$ state of $Fe(H_2O)^+$ is a few kcal/mol *above* its $^6A_1$ state. However, upon addition of the *second* H_2O ligand the situation changes dramatically in that the calculated $^4B_{1g}$ ground state of $Fe(H_2O)_2^+$ is more than 20 kcal/mol below the available sextet states. Quite clearly, in the adiabatic hydration of Fe^+ – as well as in its reverse process [27] – spin–orbit coupling must play a decisive role.

Effects of spin-surface crossing on the kinetics of sequential ligation of Ru^+ with ammonia, Eq. (18), were reported recently by Bohme and co-workers [29]. Selected ion flow tube experiments, complemented by DFT calculations of ligation free energies for the sequential ammonia ligation of ground-state $Ru^+(^4F)$ and of excited $Ru^+(^2D)$ indicate a discontinuity in the relative ligation free energy that implies a quartet → doublet spin conversion upon the addition of the *fourth* NH_3 molecule. The ligation free energy for this step amounts to $\Delta G_{298} = -18.8$ kcal/mol for generating a doublet state and to only −6.4 kcal/mol to form, in a spin-conserving process, a quartet state of $Ru(NH_3)_4^+$. Since the *rate* of ligation inter alia is dependent on the *free energy* of ligation, the observed increase in rate constant by nearly one order of magnitude, Eq. (18), points to an efficient spin–orbit coupling, the actual amount of which is, however, unknown.

$$Ru^+(^4F) \xrightarrow[k_1]{NH_3} Ru(NH_3)^+(s=3/2) \xrightarrow[k_2]{NH_3} Ru(NH_3)_2^+(s=1/2)$$

$$\xrightarrow[k_3]{NH_3} Ru(NH_3)^+(s=3/2) \xrightarrow[k_4]{NH_3} Ru(NH_3)_4^+(s=1/2) \quad (18)$$

$k_1 = 7.7 \times 10^{-12}$, $k_2 = 3.6 \times 10^{-10}$, $k_3 = 5.3 \times 10^{-11}$, $\boldsymbol{k_4}$ = **3.6×10^{-10} cm^3 molecule^{-1} s^{-1}**.

Spin aspects have also been made responsible for the kinetics of the ligand association/dissociation gas-phase chemistry of *neutral* transition-metal complexes, and the textbook case of CO association with $Fe(CO)_n$ (n = 3 and 4) fragments may serve as an example, Eqs. (19) and (20) ([30]).

$$Fe(CO)_3 + CO \rightarrow Fe(CO)_4 \quad (19)$$

$$Fe(CO)_4 + CO \rightarrow Fe(CO)_5 \quad (20)$$

While reaction (19) proceeds essentially at the collision rate, addition of CO to $Fe(CO)_4$ is by a factor of 500 slower. As the rate of reaction (20) is not appreciably temperature dependent, this difference in rates between these two seemingly similar association reactions cannot be blamed on the existence of a barrier for reaction (20). However, $Fe(CO)_3$ and $Fe(CO)_4$ have triplet ground states, whereas the 18 electron complex $Fe(CO)_5$ is a singlet. Obviously, reaction (19) is spin-allowed, while the addition of the next CO ligand is spin-forbidden, and the spin–orbit coupling is not sufficiently efficient to accelerate the crossing of the two potential energy surfaces. Many other reactions exhibiting similar features have been studied, e.g., the associations of $Fe(CO)_4$ with ligands such as H_2, C_2H_4, N_2 [31]. Clearly, spin aspects do matter! This is also corroborated by the generally sluggish, if not absent, reactivity in the association of bare *neutral* 3d atoms with alkanes and alkenes [3d], and a discussion of the Ni/C_2H_4 system may suffice. Bonding in a metal–alkene complex follows the conventional Dewar–Chatt–Duncanson mechanism [32] which is characterized by the simultaneous formation of two donor–acceptor bonds (Fig. 2). The σ-bond involves donation of electrons from the olefin 2pπ orbital to the empty metal 4s orbital along the axis of C_{2v} approach, and the π-bond forms by 'back-donation' of electrons from the metal $3d_{xz}$ orbital to the empty 2pπ* orbital of C_2H_4. Obviously, the Ni ground state has both the wrong orbital oc-

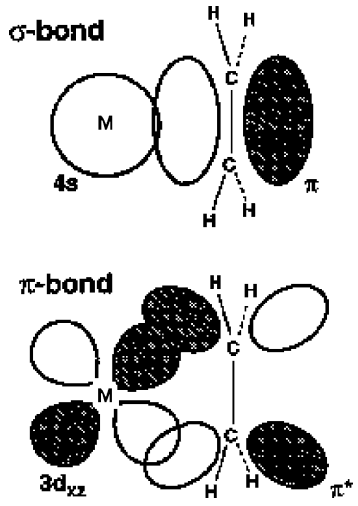

Fig. 2. Donor–acceptor model of M–C_2H_4 bonding, showing both σ- and π-bonds, according to Ref. [32].

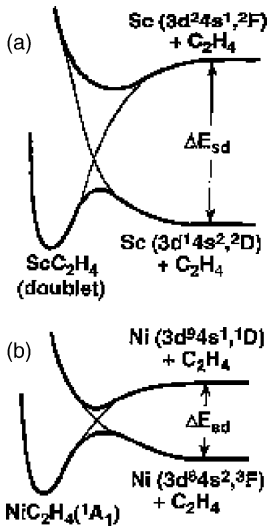

Fig. 3. Simplified potential energy curves for the approach of atomic Sc (a) and Ni (b) to C_2H_4 in C_{2v}-symmetry. Bold lines are adiabatic curves, and light lines are diabatic curves that conserve electron spin and metal configuration. The two diabatic curves have the same electron spin for Sc but different spin for Ni. Reproduced from *Acc. Chem. Res*. 26 (1993) 213.

cupancy ($4s^2$ instead of empty 4s) and the wrong spin (triplet instead of singlet) to form strongly-bonded NiC_2H_4 in its singlet state ($^1A_1$) [33].

However, $3d^84s^2 \rightarrow 3d^94s^1$ promotion permits sd hybridization of Ni, and this hybrid allows to form the new bonds in the NiC_2H_4 complex [33,34]. While the interaction of C_2H_4 and the ^3F ground state of Ni results in a *diabatic* repulsive potential energy surface (Fig. 3), the $3d^94s^1(^1D)$ excited state is well suited to bind to C_2H_4 and it provides diabatic surfaces that are *attractive*. Crossing of the two diabatic surfaces of different spin will be weakly avoided and spin–orbit coupling will generate two new *adiabatic* surfaces, shown as the bold lines in Fig. 3. On the lower adiabatic surfaces, the electron configuration and electron spin changes smoothly in the course of the reaction. In a first approximation, the barrier of the reaction has been related to the s → d promotion energy, and the latter can be approximated by the atomic's excitation term ΔE_{sd} [35]. Ni reacts efficiently because ΔE_{sd} amounts only to 6 kcal/mol, compared with 67 for Mn, 34 for Fe, and 20 kcal/mol for Co, metals which are inert at 300 K. Observation of the NiC_2H_4 formation at this temperature implies an *adiabatic* barrier height no larger than 5 kcal/mol, which correlates well with a calculated 10 kcal/mol barrier for the *diabatic* curve crossing above ground-state reactants.

The reason why atomic Sc, Ti and V – despite their large ΔE_{sd} which are comparable to the excitation energies of the inert metals Mn, Fe, and Co – react slowly with C_2H_4 is due to the fact that these 'early' transition metals need not change their electron spin to bind to C_2H_4 (Fig. 3a for Sc). As crossing of diabatic surfaces of the same spin will be more strongly avoided than crossing between surfaces of different spin, for a given ΔE_{sd} value one can reasonably expect smaller adiabatic barrier heights and, consequently, enhanced reactivity.

3.2. The bond activation step: some general considerations

Why do atomic transition-metal cations M^+ from the left-hand side ('early' metals) of the 3d block preferentially attack C–H bonds of alkane, while those on the right hand of the periodic table ('late' metals) activate both C−H and C−C bonds? How to account for the observation that excited states of some 3d cations are more reactive than the ground states (e.g., Ti^+, V^+, Cr^+, Mn^+, Fe^+), while the opposite holds true for other metals (e.g., Co^+, Ni^+, Cu^+)? Obviously, energetics alone is not the dominant factor in determining reactivity. Also counter intuitive is the observation that for some transition-metal cations the product distribution MH^+ versus MD^+ in the reactions of M^+ with HD is strongly affected by the particular electronic and spin states of M^+. Further, how does it come that electronic excitation of Fe^+ to its ^4F states brings about rate acceleration (in comparison to the electronic ground state ^6D), while the branching ratios, for example C−H versus C−C bond activation of a particular substrate, were essentially identical for all electronic states examined? No doubt, the repeated observation that differences in electronic energy and spin multiplicities affect rate constants but *not* branching ratios is inconsistent with a picture invoking perfectly separated hypersurfaces for each spin state—and there are sometimes many: In the reaction of H_2 with Sc^+, for example, there exist 65 low-lying spin and angular momentum components for Sc^+ that might contribute to the reaction via each of two (parallel versus perpendicular) reaction geometries [36]. In practice, however, only a few states are important at low energies and spin may not always be a good quantum number.

Despite the mounting evidence for the relationship between spin aspects and chemical reactivity, the crucial role of spin inversion was often neglected, if not regarded as inappropriate, in particular for a mechanistic description of reactions in organometallic chemistry [37]. Although the necessity to explicitly consider 'surface hopping' as a mechanistically decisive step in metal-mediated chemical transformations was pointed out more than a decade ago [3a,3b,3c,3d,32,38], the assumptions of either strict spin conservation or its complete neglect pervaded many chemistry and physics textbooks. But pioneering experiments, notably from the laboratories of Armentrout, Beauchamp, Bowers and Weisshaar, in conjunction with thorough theoretical analyses, have changed the picture. It is now recognized that it is the subtle interplay of electronic and kinetic energy, the effect of spin and spin–orbit coupling efficiency, as well as the electronic configuration of M^+, which determines the course and outcome of bond activation by a bare transition-metal ion according to Eq. (17). Of course, this also holds true for the gas-phase chemistry of neutral [3d] and doubly-charged [39] metal atoms.

Some of the characteristic features of an elementary process will be discussed in the next chapter that deals with the deceptively simple cleavage of a H−H bond, i.e., reaction (21), and reactions (21a) and (21b) for the H−D variant of molecular hydrogen.

$$M^+\left(s \pm \tfrac{1}{2}\right) + H_2(0) \rightarrow MH^+(s) + H\left(\tfrac{1}{2}\right) \quad (21)$$

$$M^+ + HD \rightarrow MH^+ + D \quad (21a)$$

$$M^+ + HD \rightarrow MH^+ + H \quad (21b)$$

3.3. Reactions of atomic M^+ with molecular hydrogen

Activation of H_2 by an atomic transition-metal ion M^+ (or any atomic ion [40a]) is controlled by a combination of molecular orbital (MO) and spin considerations as well as spin–orbit coupling [3a,b,c]. Based on work by Mahan [41] and Elkind and Armentrout [42], H_2 bond cleavage can be viewed as a process in which the bonding electrons of H_2, $\sigma_g(H_2)$, are donated to the metal centre, which in turn donates electrons into the anti-bonding orbital of H_2, $\sigma_u^*(H_2)$, thus weakening the H−H bond. For atomic metal ions, the primary acceptor orbital is the s orbital (with contributions from dσ), while the donor is a doubly-occupied dπ orbital. If the s orbital is occupied, the state is relatively unreactive. The most reactive species are those in which both the s and the dσ orbitals are empty, as in 'early' transition metal ions having orbital configurations ($s^0d\pi^2$) that should lead directly to the formation of ground state MH_2^+. A related consideration concerns the role of electronic spin, which is easily conserved *overall* in Eq. (21) (where the spin quantum numbers are given in parentheses) since M^+ can be in either of two spin quantum numbers ($s \pm 1/2$) and still forms ground states $MH^+(s)$ in a spin-allowed process. For example, ground-state FeH^+ ($^5\Delta$, s = 2) [43] can be generated from both $Fe^+(^6D)$ and $Fe^+(^4F)$; however, the favourable $s^0d\pi^2$ configuration can only be achieved for low-spin ($s - 1/2$) metal ion states, e.g., $Fe^+(^4F, 3d^7)$. High-spin states, resulting from $s^1d\pi^1$ etc., e.g., $Fe^+(^6D, 4s3d^6)$ should have PESs that are more repulsive. In addition, they can only access ground state intermediates via spin–orbit coupling. That not only the overall spin of reaction (21) but the spin of the *reaction intermediate*, i.e., H−M^+−H, needs to be considered is also verified by the reactivity of other metal ions. For $M^+ = Cr^+$, the quartet states react more readily than the sextet state [44], and as the product CrH^+ has a $^5\Sigma$ ground state [38,43–45], reaction (21) is spin-allowed for *both* states of Cr^+. However, when the reaction proceeds via an intermediate H−Cr^+−H, a spin change is necessary for high-spin Cr^+, because formation of ground-state intermediates is only spin-allowed for the low-spin metal. This consideration also explains why *excited* states of Co^+, Ni^+ and Cu^+ – in spite of their extra excitation energy – are *less* reactive than the ground states. For these three metal cations, the ground states are low-spin thus not relying on efficient spin–orbit coupling in the oxidative insertion. As first elucidated by Elkind and Armentrout [40b] and later summarized by Armentrout and Beauchamp [3a], based on these relatively simple ideas, three categories of reactivity exist for 3d transition metal cations: (1) States such as $Ti^+(^4F, 3d^3)$ react efficiently, and based on the reactions with HD, the nearly 1:1 ratio in the formation of TiH^+ and TiD^+ (Fig. 4a) indicates a statistical behaviour of the H−Ti^+−D intermediate. This situation seems to hold true in general for metal ions with $3d^n$ ($n < 5$) configurations [40a]. (2) If either the 4s or 3dσ orbital is occupied and the ion is low-spin, the systems react via a *direct* reaction mechanism. The behaviour of the low-lying excited state $Fe^+(^4F, 3d^7)$, Fig. 4b, is typical, and the product distribution favouring the formation of FeH^+ over FeD^+ is controlled by angular momentum conservation [40a,46]. (3) If either the 4s or 3dσ orbital is occupied and the ion is high-spin, the systems react very inefficiently, consistent with the repulsive surfaces predicted by the MO concept. Ground-state $Fe^+(^6D, 4s3d^6)$ is an example. The reaction commences at an elevated threshold and produces much more FeD^+ than FeH^+ which is indicative for an *impulsive* behaviour [40a]. Obviously, in the Fe^+/HD system, the two electronic states of the metal must react with HD through entirely different reaction mechanisms which reflect state-specific features. Of course, mixing of PESs (i.e., non-adiabatic effects) can bring about changes in reactivity. For example, the category 3 ions of Sc^+ and Ti^+ having ground states $Sc^+(^3D, 4s3d)$ and $Ti^+(^4F, 4s3d^2)$, were observed to react like category 1 ions, i.e., $Sc^+(^3F, 3d^2)$ and $Ti^+(^4F, 3d^3)$ because the *repulsive* ground-state PESs undergo strongly avoided crossings with the *attractive* excited-states of identical electronic spin [47].

As a final example of this Chapter some aspects of the fascinating Sc^+/H_2 couple will be mentioned; this system has met the interest of theoreticians [36,38] and experimentalists [47b,48] alike. Atomic $Sc^+(^3D, 4s3d)$ is by far the most reactive of the 3d metal ions [46,49]. *Exothermic* insertion of Sc^+ into H_2, forming two Sc−H σ-bonds, was first predicted by Tolbert and Beauchamp [48a], and the ability to generate exothermically metal hydride bonds was attributed to the fact that the 3d4s configuration of Sc^+ allows the formation of two equivalent sd hybrid bonding orbitals and greatly reduces the loss of exchange energy on the metal in the course of σ-bond formation. This exothermic insertion distinguishes Sc^+ from other metal cations, e.g., Co^+, V^+, Na^+ or K^+, all of which bind a hydrogen molecule mainly by electrostatic forces [50], resulting in a complex in which the H_2 bond is only slightly perturbed from the isolated molecule [51]. At elevated kinetic energy, reaction of Sc^+ with H_2 under single-collision conditions brings about H−H bond cleavage, according to Eq. (21) [46,47b,52]. Detailed theoretical work [36,38] helped to uncover part of the uniqueness of Sc^+. The inserted $Sc(H)_2^+$ structure was confirmed to correspond to the ground state ($^1A_1$), and the intermediate is

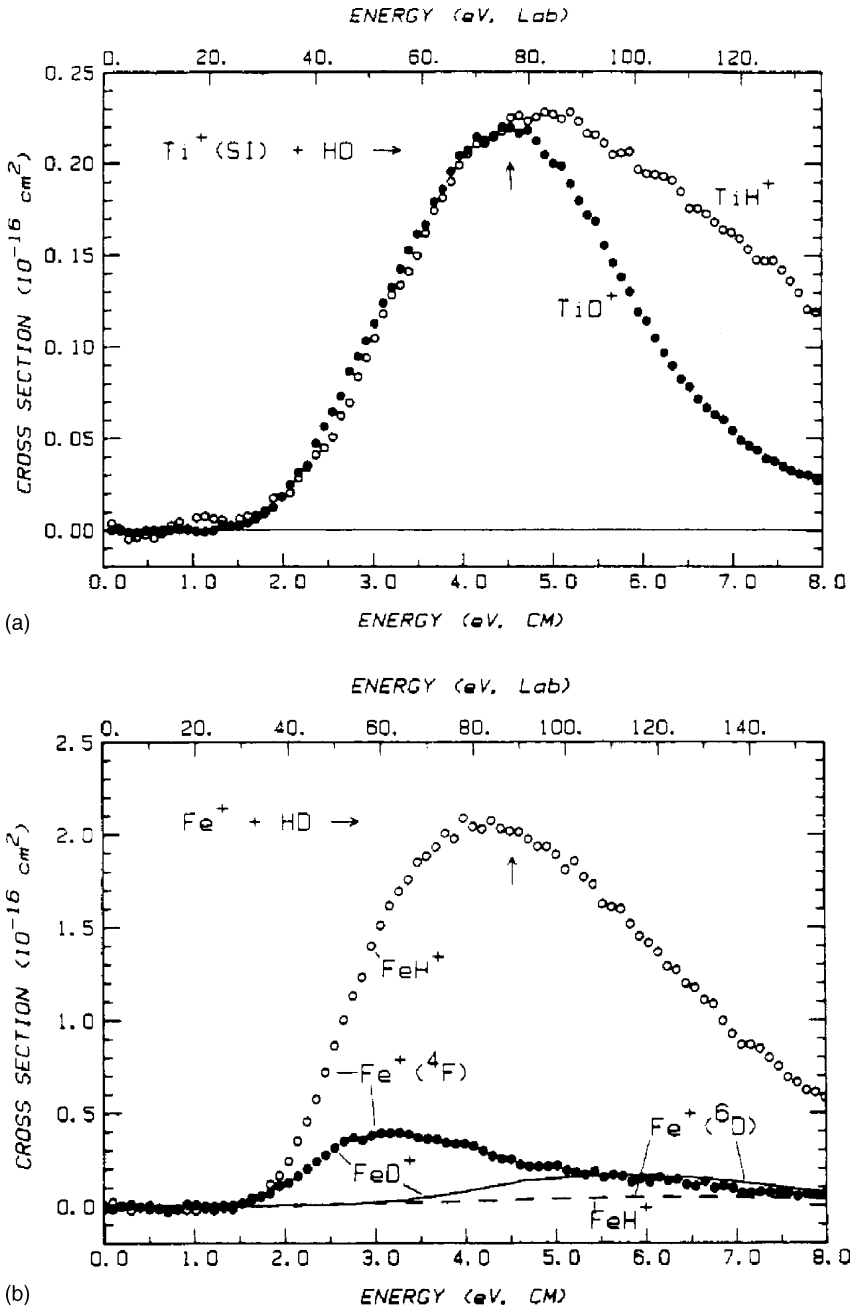

Fig. 4. Cross-sections for the reactions of (a) Ti^+ and (b) Fe^+ with HD (Eqs. (21a) and (21b)) as a function of collision energy in the laboratory (upper scale) and centre-of-mass (CM, lower scale) frames. Reproduced from *Acc. Chem. Res.* 22 (1989) 315.

formed adiabatically from a low lying first excited state (^1D, 4s3d) through an avoided crossing with the third excited state (^1D, 3d^2). The effects of spin–orbit coupling between surfaces of $Sc(H)_2^+$ that correlate to the atomic ground state of Sc^+(^3D, 3d4s) and the two first excited ^2D states were estimated. While the calculations indicated that formation of an inserted $H{-}Sc^+{-}H^+$ structure was probably exothermic with respect to the Sc^+ ground state asymptote, a large barrier of 19 kcal/mol will prevent facile bond activation. Some relevant parts of the potential energy curves are depicted in Fig. 5.

Additional insight on the details of σ-bond activation of H_2 by Sc^+ was provided in a combined experimental/theoretical approach by Bowers and co-workers [48b] using temperature-dependent equilibrium measurements for reaction (22).

$$Sc(H_2)_{n-1}^+ + H_2 \rightleftharpoons Sc(H_2)_n^+ \quad (22)$$

Both experimental and theoretical analyses of the data indicate that Sc^+ is inserted exothermically into the first H_2 ligand although the rate is very slow (k = (3–13) × 10^{-17} cm^3 s^{-1}). More interestingly, this rate constant has a

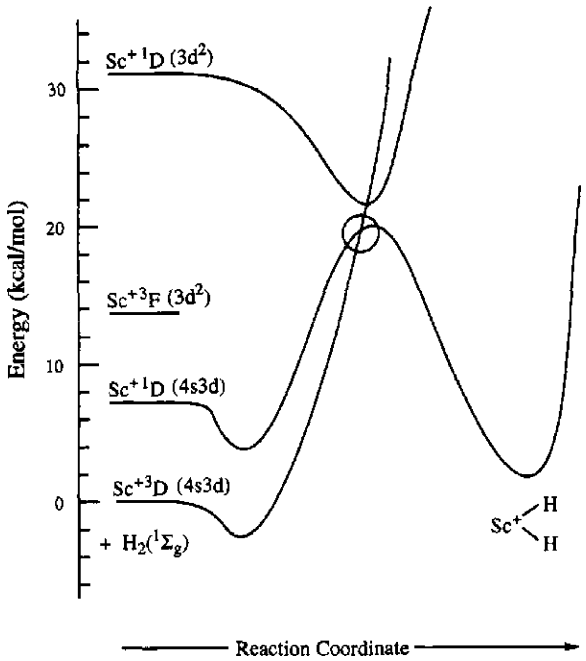

Fig. 5. Potential energy curves modelled after the results of Rappé and Upton (Ref. [36]) for the C_{2v} approach of atomic Sc^+ and H_2. The two ^1D states undergo an avoided crossing, allowing an entry to the formation of $Sc(H)_2^+$ ($^1A_1$). The circle denotes a spin–orbit mediated coupling between the ^3D ground state and the first excited ^1D state. Reproduced from *J. Am. Chem. Soc*. 116 (1994) 9710.

negative temperature dependence which is incompatible with a simple insertion energy barrier as suggested in Fig. 5 for the reaction occurring under single-collision conditions between Sc^+ and H_2.

The negative temperature dependence requires to have the rate-determining transition state be at slightly *lower* energy than the ground state asymptote energy. How can this be achieved? Bowers and co-workers provided a convincing rationale by theoretically examining the effect of sequential H_2 clustering on various energy states of Sc^+. In the present context the important finding is that sequential addition of H_2 molecules to these states leads to a lowering of the insertion barrier relative to the asymptotic energy of the ground state [Sc^+ ^3D, 4s3d, + nH_2], and it takes *three* H_2 molecules to pull the insertion barrier below the asymptotic limit. Obviously, it is *not* the bare Sc^+ ion that brings about H−H bond activation but the cluster ^3D $Sc^+(H_2)_2$ which, upon ligation with a third H_2 molecule, is ready to undergo formation of the inserted H−Sc^+−$H(H_2)_2$ intermediate and eventually the H−Sc^+−H product itself. This oxidative addition is a rare example of a cluster-mediated σ-bond activation.

3.4. Bond activation of XH_4 (X = C, Si) and small aliphatic hydrocarbons by bare M^+

Methane functionalization constitutes an important, timely topic of research [53], and catalytic conversion of CH_4 to CH_3OH has been listed as one of the ten challenges of contemporary catalysis [54]. Not surprisingly, methane activation by bare transition-metal cations has been at the focus of a number of fundamental gas-phase ion studies [3d,55]. While several electronically excited ions M^+ were reported to dehydrogenate methane [56], reaction (23), and to form metal-carbene complexes MCH_2^+, thermalized ground-state mono-atomic 3d- and 4d-elements do not react with methane (atomic Zr^+ seems to be an exception in that in guided ion beam experiments at low energies slightly *endothermic* dehydrogenation of CH_4 has been observed) [3a,3d,57].

$$M^+ + CH_4 \rightarrow MCH_2^+ + H_2 \quad (23)$$

Interesting ‘exceptions’ to the generally non-reactive behaviour of 3d- and 4d-cations towards CH_4 were recently reported using quite different concepts. For example, Bowers and co-workers demonstrated that methane activation can be achieved by means of a ‘ligand-assisted’ reaction [58]. Bondybey’s laboratory reported that dimeric Rh_2^+, in distinct contrast to atomic Rh^+ as well as larger clusters, efficiently dehydrogenates CH_4 [59a], and the same reaction is observed for the heteronuclear clusters $RhPt^+$ [59b] and, with small efficiency, $RhCu^+$ (M. Schlangen, H. Schwarz, unpublished results). Further, a detailed analysis of the gas-phase performance of Bergman’s catalyst [53e] with regard to methane activation was conducted by Chen and co-workers [60].

The unreactivity of bare metal ions, especially from the first row, is due to the repulsive properties of the occupied 4s orbital and unfavourable thermodynamics, and it takes third-row transition-metal cations M^+ (M = Ta, W, Os, Ir, Pt) to make reaction (23) exothermic, as demonstrated for the first time by Irikura and Beauchamp [61] and later confirmed by other laboratories [55b]. In these cases, reaction (23) is driven by the formation of extraordinarily strong metal–carbene bonds ($D_0(M^+{-}CH_2)$ >111 kcal/mol), and these remarkable bond strengths can be attributed to relativistic stabilization of the cationic complexes MCH_2^+ [62]. Similar effects exist for the chemistry of homo- and heteronuclear cationic clusters composed of platinum and coinage metals, some of which exhibit unusual cluster size effects for reaction (23) [63].

A question of obvious interest is whether the electronic and spin considerations so crucial for the activation of H_2 by 3d- and 4d-metal cations M^+, Eq. (21), continue to play a role for alkanes as well.

Methane is the simplest system where *endothermic* C−H bond cleavage can be studied, Eq. (24), and ethane and propane extend this to the competitive activation of a C−C bond. Possible spin quantum numbers in the metal-mediated reactions of CH_4 are given in parentheses of Eq. (24).

$$M^+(s \pm ½) + CH_4(0) \rightarrow \begin{cases} MCH_2^+ (s\text{-}½) + H_2(0) & (24a) \\ MH^+ (s) + CH_3(½) & (24b) \\ MCH_3^+ (s) + H(½) & (24c) \end{cases}$$

State-specific results for the ion–molecule processes of excited Ti^+, V^+, Cr^+ and Fe^+ with methane indicate that the MO concepts discussed above for H_2 activation remain valid for the cleavage of C−H bonds [49,52,56b,64], and the three categories of reactivity pattern derived can be applied. Reactions (24a)–(24c) all take place for Sc^+−Cr^+, this is indicative for the formation of a long-lived intermediate H−M^+−CH_3. Fe^+ does not dehydrogenate CH_4, Eq. (24a), but undergoes reactions (24b) and (24c) which suggest direct processes, and the ^4F state of Fe^+ is much more reactive than the ^6D ground state in generating FeH^+. For the Fe^+/CH_4 system recent extensive computational studies [65] do not only agree nicely with most of the experimental findings, but also reveal a crucial detail with regard to the spin-crossover. In disagreement with the previous assignment of a sextet state to the $FeCH_4^+$ complex [66], the ground state of the complex is characterized by a quartet spin state with a binding energy that is consistent with the measured value [67] and other high-level computational findings [68]. Thus, the crossing point occurs quite likely at the entrance channel and the system stays on the quartet surfaces without any changes in multiplicities. As dehydrogenation, reaction (24a), is associated with an energetically substantial and entropically demanding barrier in excess to endoergicity, it is not surprising that the Fe^+/CH_4 couple prefers formation of FeH^+ and $FeCH_3^+$ the spin-dependent branching ratio of which is, to some extent, also controlled by angular momentum conservation [64c,69]. Alternatively, it can be argued that FeH^+ is formed in a direct 'stripping' reaction proceeding via a colinear M^+−H−CH_3 intermediate [3a]. For the Ti^+/CH_4 system [64b], the study of the electronic and translational energy dependence augmented by extensive qualitative MO considerations provides good support for the idea that the endothermic formation of TiH^+ and $TiCH_2^+$ proceeds primarily through a doublet H−Ti^+−CH_3 intermediate which is efficiently populated from the s ^2F excited state of the metal ion; this state is significantly more reactive than the a ^4F ground and b ^4F first excited states of Ti^+. As the latter states also dehydrogenate CH_4, and as this process is spin-forbidden for these two quartet states, the doublet intermediate H−Ti^+−CH_3 is accessed via spin–orbit coupling of the doublet and quartet surfaces.

The last example to be discussed in this Chapter concerns the reactions of the 'early' 3d cation Sc^+ with CH_4, which has been studied by guided ion beam mass spectrometry [52] and thoroughly analyzed theoretically at different levels of theory [62h,70].

At low kinetic energy of Sc^+, the dominant process corresponds to dehydrogenation, Eq. (24a) (M = Sc); at higher energy the cross-section of this reaction falls off as the cross-sections for the formations of ScH^+ (Eq. (24b)) and $ScCH_3^+$ (Eq. (24c)) rise, with the former one predominating (Fig. 6) [52]. The smooth appearance of the total cross-section suggests that reactions (24a) and (24b) are closely coupled, and the decline of the $ScCH_2^+$ product above 1.9 eV must be a result of competition with the other two processes, because $ScCH_2^+$ cannot decompose until 4.8 eV. Qualitative MO considerations [52] suggest a quite complex potential energy surface due to the existence of various electronic states of Sc^+ [36] and the fact that the hypothetical intermediate H−Sc^+−CH_3 must correspond to a singlet ground state. This conjecture has been validated in two extensive high level ab initio [62h] and density functional (DFT) theory [70] calculations (Fig. 7).

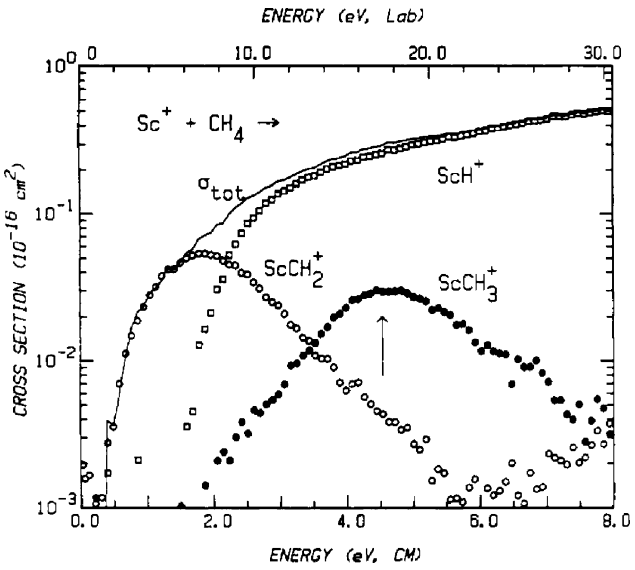

Fig. 6. Variation of product cross-sections with kinetic energy of Sc^+ in the laboratory frame (upper axis) and centre-of-mass frame (lower axis). The arrow indicates D^0(H−CH_3) at 4.54 eV. Reproduced from *J. Am. Chem. Soc.* 111 (1989) 3845.

According to Morokuma's multi-reference studies [62h], which compare favourably with DFT-derived findings [70] and exhibit good agreement with available experimental data [48a,52], the reaction of the ground state Sc^+ with CH_4 proceeds as $Sc^+(^3D, s^1d^1)$ + CH_4 → $ScCH_4^+(^3A'')$ → $TS2(^1A')$ → $HScCH_3^+(^1A')$ → TS1 → $(H_2)ScCH_2^+(^1A_1)$ → $ScCH_2^+(^1A_1)$ + H_2 and is calculated to be endothermic by 24.8 kcal/mol. After formation of an ion–molecule complex $ScCH_4^+$, the reaction cannot continue on the triplet surface because of a high barrier; rather it has to cross over to the singlet surface. The minimum energy crossing point, denoted by XM in Fig. 7 and corresponding to a η^3C_{2v} structure, is located some 10 kcal/mol above the $ScCH_4^+$ triplet complex but still 13 kcal/mol below singlet TS2. The latter is 28.6 kcal/mol above the entrance channel. From the crossing point onwards the system stays on the singlet potential energy surface. Thus, the reaction of the first excited state of $Sc^+(^1D, s^1d^1)$ is predicted [62h] to take place more easily, because of extra initial electronic energy and because it would not require the intersystem crossing via rather inefficient spin–orbit coupling. On the other hand, as outlined above, occupation of an s orbital gives rise to a repulsive interaction and the metal is not expected to insert easily into a C−H bond. In any case, from the insertion product $HScCH_3^+$ the reaction branches out into three different channels (reactions (24a)–(24c), with M

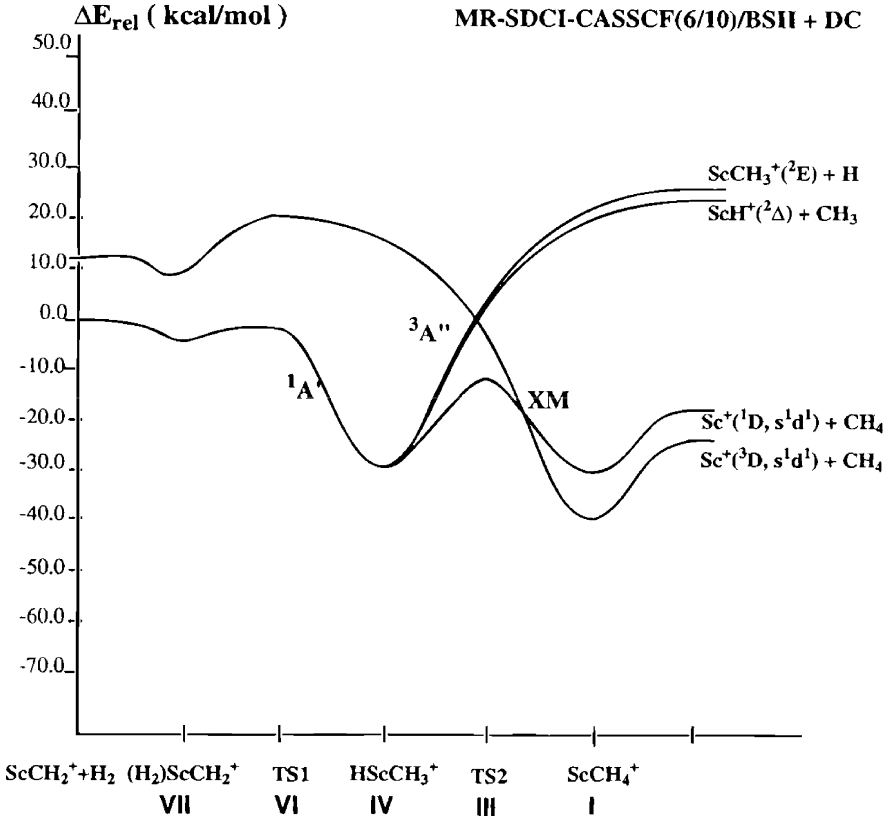

Fig. 7. Potential energy profiles for the Sc^+/CH_4 system calculated at the MR-SDCI-CASSCF(6/10)/BSII + DC level. Reproduced from *J. Phys. Chem.* 28 (1996) 11600.

= Sc). The energetically most favoured process corresponds to dehydrogenation and formation of $ScCH_2^+$; this path is clearly preferred at low kinetic energies as observed experimentally [52]. Productions of ScH^+ and $ScCH_3^+$ are energetically more demanding; however, both channels have an entropic advantage ('loose' transition states), and are therefore easier accessible at higher kinetic energies. In addition, a small fraction of the ScH^+ product may be formed in a direct process via a colinear Sc^+-H-CH_3 alignment, as suggested earlier [52], thus bypassing formation of the insertion intermediate. This direct reaction is spin-allowed from both high- and low-spin states of Sc^+.

Before continuing with a discussion of the gas-phase chemistry of bare M^+ with C_2H_6 and C_3H_6, which serve as representative examples for competitive C−H/C−C bond activation, brief comparison of CH_4 with its heavier analogue SiH_4 should be made with an emphasis on mechanistic aspects of the Si−H bond cleavage steps by the 3d metal cations Sc^+ [71], Ti^+, V^+, Cr^+ [72], and Fe^+, Co^+, Ni^+ [73]. Common to these guided ion beam studies is an attempt to unravel the role of electronic excitation, molecular orbital concepts and spin considerations on the cross-section as a function of kinetic energy.

For the Sc^+/SiH_4 couple the major low-energy process corresponds to formation of $ScSiH_2^+ + H_2$, Eq. (25), while at higher energies the products ScH^+/SiH_3 and ScH_2^+/SiH_2 dominate. The overall reactivity is greater in the silane system compared to Sc^+/CH_4. Not unexpectedly, the $Sc^+(a^3D)$ ground state is an order of magnitude less reactive than the $Sc^+(a^1D, a^3F)$ states, and formation of ScH_2^+/SiH_2, which is entirely absent in the Sc^+/CH_4 couple, is only observed for reaction of SiH_4 with $Sc^+(a^1D)$. All these findings can be understood in terms of simple MO and spin conservation concepts, as discussed above for the Sc^+/CH_4 system, and augmented by the fact that (i) the Si−H bond is significantly weaker than a C−H bond and (ii) the enhanced hydrogen mobility at silicon centres [74].

The singlet insertion product $H-Sc^+-SiH_3$ is suggested to act as common intermediate for most of the products formed. While spin–orbit coupling, not unexpectedly, is quite inefficient for Sc^+, the increased reactivity of the heavy metal La^+ in its reaction with SiH_4 [71] has been attributed to a much more efficient spin–orbit coupling between the unreactive high- and the reactive low-spin surfaces.

Similar observations were reported for the reactions of $M^+ = Ti^+$, V^+, and Cr^+ with SiH_4 [72], with $MSiH_2^+$ as the major product at lower translational energies and the formation of MH^+/SiH_3 at higher energies. Further, the reactions are more efficient for the low-spin doublet (Ti^+), triplet (V^+), and quartet (Cr^+) excited states of the metal ions, and this probably explains why dehydrogenation exhibits the largest enhancement for the three metal cations. Spin-consideration shows that reaction (25) is spin-allowed for low-spin but not high-spin states of M^+ [75]. Consequently, the experi-

mental observation that the high-spin ground states of Ti^+, V^+ and Cr^+ react with SiH_4 to form $MSiH_2^+/H_2$ implies that spin–orbit coupling between the high- and low-spin surfaces is operative. However, the relative inefficiency of the ground-state reactions compared with the low-spin excited state demonstrates that, like for Sc^+, coupling is rather poor also for Ti^+, V^+ and Cr^+. Basically the same holds true for the chemistry of SiH_4 with the 'late' transition metal ions Fe^+, Co^+, and Ni^+ [73].

$$M^+\left(s \pm \tfrac{1}{2}\right) + SiH_4(0) \rightarrow MSiH_2^+\left(s - \tfrac{1}{2}\right) + H_2(0) \quad (25)$$

Let us now return to a discussion of some aspects of hydrocarbon chemistry. As mentioned above, the metal-mediated reactions with ethane (and propane) are ideal to probe one of the central challenges in this field, i.e., the competition between C−H and C−C bond activation. Earlier work has been summarized in Refs. [3a,3b,3d,25], and some more general aspects relevant to the topics addressed in this Review will be discussed here. In addition, brief attention will be paid to a few original publications [76–78] which highlight part of the fundamental problems associated with these seemingly simple bond activation processes.

For C_2H_6 depending on the metal cation and its translational energy, reactions (26a)–(26g) have been observed, and both the efficiencies and the branching ratios are highly metal specific.

$$M^+ + C_2H_6 \rightarrow \begin{cases} MCH_3^+ + CH_3 & (26a) \\ MCH_2^+ + CH_4 & (26b) \\ MC_2H_4^+ + H_2 & (26c) \\ MH_2^+ + C_2H_4 & (26d) \\ MC_2H_2^+ + 2H_2 & (26e) \\ MH^+ + C_2H_5 & (26f) \\ MH + C_2H_5^+ & (26g) \end{cases}$$

Expulsions of CH_3 and CH_4, reactions (26a) and (26b), involve C−C bond cleavage, and process (26a) dominates at high translational energy for all metal ions investigated. Demethanation is observed only for the 3d metals Sc^+−Cr^+, and as these two C−C bond activation processes compete, it has been suggested that they proceed through a common insertion intermediate $M(CH_3)_2^+$ which eliminates CH_4 via a tight four-centre transition state or CH_3 via direct metal-carbon bond fission. All remaining reactions involve at one stage C−H bond activation. Processes (26f) and (26g) dominate again at higher translational energy, and they can occur directly from an insertion intermediate $H-M^+-C_2H_5$. Not surprisingly, their branching ratio will be controlled by the ionization energies of MH and C_2H_5. While dehydrogenation, reaction (26c), is exothermic for all 3d cations it is not observed for Cr^+, Mn^+ or Cu^+ but occurs for Fe^+, Co^+, and Ni^+ though with substantial activation barriers. In contrast, the 'early' transition metals Sc^+, Ti^+, and V^+ show no barrier and exhibit large cross-sections for dehydrogenation of C_2H_6. In general, the cross-sections of reaction (26c) are dependent on the spin state of the metal: low-spin states are more efficient than high-spin states [76,79]. Formation of MH_2^+ is observed uniquely for metal ions with two valence electrons, i.e., Sc^+, Y^+, La^+, and Ln^+ [52], and the exclusive formation of $ScHD^+$ from CH_3CD_3 is indicative for highly specific consecutive C−H(D) bond activation steps, the efficiency of which, however, is rather low due to the inefficient spin–orbital coupling between the triplet-singlet surfaces. If the rate limiting step for reactions (26a)–(26g) is insertion of M^+ into a C−H or a C−C bond, then electron spin conservation and electronic occupancy restrict which reactant states provide under low-energy collisions a low-energy path for the M^+/alkane system to the intermediate. Again, ions in low-spin states quite generally have a spin-allowed entry while those with high-spin ground state have an efficiency which is subject to spin–orbit coupling.

With larger alkanes, many of their reactions with transition-metal cations exhibit *exothermic* features with cross-sections approaching the collision limit near thermal energies. Further, crossings between surfaces of different metal ion states (including different spins) often occur at energies *below* the reactant asymptote such that the reactions can be largely insensitive to spin considerations. In general, the difference in reactivity between ground and excited states is often seen to decrease as the system evolve from small to larger sizes. This is due to an increase of reactivity of the ground states rather than the excited states become less reactive. One might anticipate that for a sufficiently large system, all state-specific reactivity differences eventually disappear; however, this limit has not yet been reached.

As a good example for a 'larger' alkane, the reactions of M^+ with *n*-butane, Eq. (27), are perhaps instructive.

$$M^+ + n\text{-}C_4H_{10} \rightarrow \begin{cases} MC_4H_8^+ + H_2 & (27a) \\ MC_4H_6^+ + 2H_2 & (27b) \\ MC_3H_6^+ + CH_4 & (27c) \\ MC_2H_4^+ + C_2H_6 & (27d) \\ M(CH_3)_2^+ + C_2H_4 & (27e) \end{cases}$$

Again, and as expected for exothermic processes, branching ratios are highly metal specific [80], as demonstrated by the following few examples: First-row, 'late' cations readily activate C−H and C−C bonds. Metals with two valence electrons like Sc^+, are unique in that formation of $Sc(CH_3)_2^+$ is prominent [48a,81]. Ground-state Cr^+ and Mn^+ are unreactive with C_4H_{10} at low translational energy, because formation of an insertion product requires two relatively strong σ-bonds which would imply a disruption of a stable d^5 shell.

One of the most detailed gas-phase experiments ever conducted concerns the *total* cross-section determination of electronic state-specified reactions of V^+ with C_2H_6, C_3H_8, and

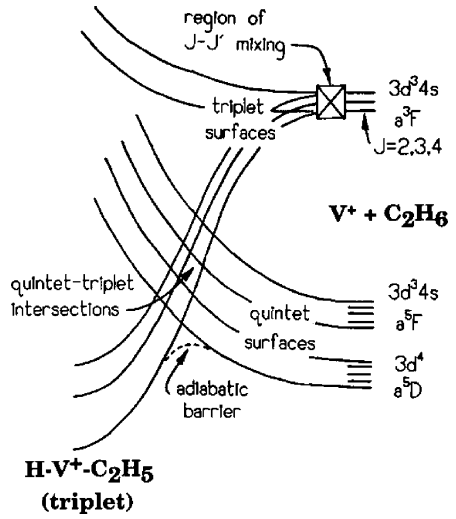

Fig. 8. Schematic representation of various V^+/C_2H_6 potential energy curves leading from quintet and triplet asymptotes towards the insertion intermediate $H{-}V^+{-}C_2H_5$. Reproduced from *J. Chem. Phys.* 92 (1990) 3498.

C_2H_4 [76]. At a kinetic energy of 0.2 eV, for all three hydrocarbons, dehydrogenation is the dominant process, and a truly dramatic dependence of cross-section on the V^+ electronic terms was observed. The second excited term, $^3F(3d^34s)$ is more reactive than either lower energy quintet term $^5D(3d^4)$ or $^5F(3d^34s)$ by a factor of $\geq$270, 80 and $\geq$6 for C_2H_6, C_3H_8 and C_2H_4 reactions, respectively. Electronic excitation to $^3F(3d^34s)$ is far more effective at promoting H_2 elimination than addition of the same total kinetic energy to reactants. Electron spin is undoubtedly *the* key determinant of the V^+ reactivity with small hydrocarbons, and the higher efficiency of triplet V^+ – in comparison to the quintet states of V^+ – is due to its ability to conserve total electron spin along paths to bring about oxidative insertion of the metal in a C−H bond. The essential details are depicted in Fig. 8, and for a thorough discussion the reader is referred to the original publication in Ref. [76a].

Further insight into the mechanistic details of competitive C−H/C−C bond activation by ground-state Ti^+ and V^+ and the factors that govern this competition was provided by an investigation of deuterium-labeled propanes, product kinetic energy release distribution, reaction cross-section determination, and qualitative considerations of potential energy surfaces of different states [77]. The major experimental findings are as follows: For ground state Ti^+, loss of H_2 and CH_4 both occur at thermal energy with reaction efficiencies of 17 and <1%, respectively. For ground-state V^+, dehydrogenation is observed at thermal energy with an efficiency of <1%, whereas demethanation requires a 0.7 eV threshold. The deuterium labelling indicates that β−H(D) transfer to form the metal propene dihydride complex constitutes the rate-limiting step for dehydrogenation while reductive elimination of CH_4 is shown to correspond to the rate-limiting event for demethanation. These observations and many other features [77] permit to construct schematic potential energy curves for the two systems, Figs. 9 and 10.

Common to either metal is that formation of the initial $H{-}M^+{-}C_3H_7$ intermediate requires a spin–orbit mediated crossing from the high-spin ground state to an excited low-spin surface. Because both Ti^+ and V^+ eliminate H_2 at thermal energies, these crossings must occur below the reactant asymptotic energies as shown in Figs. 9 and 10. In the case of Ti^+ no further spin changes are implied for producing H_2 and CH_4 and the corresponding Ti^+ complexes. As significant isotope effects are observed in the Ti^+ cross-sections at lower energies, while SOC is expected to have little isotopic dependence, the energies of the respective multi-centre transition-states [82] play a crucial role in both the overall reaction efficiency and the branching ratio, as revealed experimentally.

Similar arguments apply to H_2 elimination in the V^+/C_3H_8 reaction except that now two crossings are involved. The reaction commences on the quintet surface, crosses to a surface and returns to the quintet surface because only the latter gives rise to an overall exoergic reaction. Inspection of the PESs also reveals that for demethanation it is the last step, i.e., the reductive elimination, which is rate limiting. Further, the reactivity difference between the Ti^+ and V^+ systems is caused by a more favourable covalent bonding for Ti^+ due to facile sd hybridization, which pulls down transition states as well as intermediates involved en route to products.

The last example, to be discussed in this chapter, deals with electronic effects in competitive C−H/C−C bond activation by excited Cr^+ [78]. Cr^+ has been one of the *least* studied metal ions, largely because the stable d^5 shell of its ground state (^6S, $3d^5$) renders the metal quite unreactive [83]. This further suggests that excited states of Cr^+ having either $4s^13d^4$ or low-spin $3d^5$ configurations should be more reactive, which was later actually observed for reactions of electronically excited Cr^+ with H_2 and CH_4 [56,84]. It was also shown that in these systems bond activation can be achieved by translational excitation of electronically 'cold' Cr^+ [56b,84b]. These earlier studies were complemented by observations that tuning the electronic states of Cr^+ provides a handle for controlling the C−H/C−C branching ratios in the activation of alkanes like C_3H_8, C_4H_{10}, and C_5H_{12} [78]. While the $^6S(3d^5)$ ground state and the $^6D(4s3d^4)$ first excited state of Cr^+ activates only C−C bonds, the excited quartet states $^4D(4s3d^4)$ and $^4G(3d^5)$ bring about both C−H and C−C bond cleavage, and these remarkable selectivity effects can be explained, once more, by relatively simple concepts employing electronic state, atomic occupancy and spin–orbit coupling considerations, which are summarized in Fig. 11 [78].

Given the reasonable assumption that the Cr−H and Cr−C bonds in all initially formed insertion intermediates $H{-}Cr^+{-}CH_2R$ and $H_3C{-}Cr^+{-}R$ are covalent, there are three remaining non-bonding 3d electrons on the metal. Consequently, these species should have quartet ground states, as

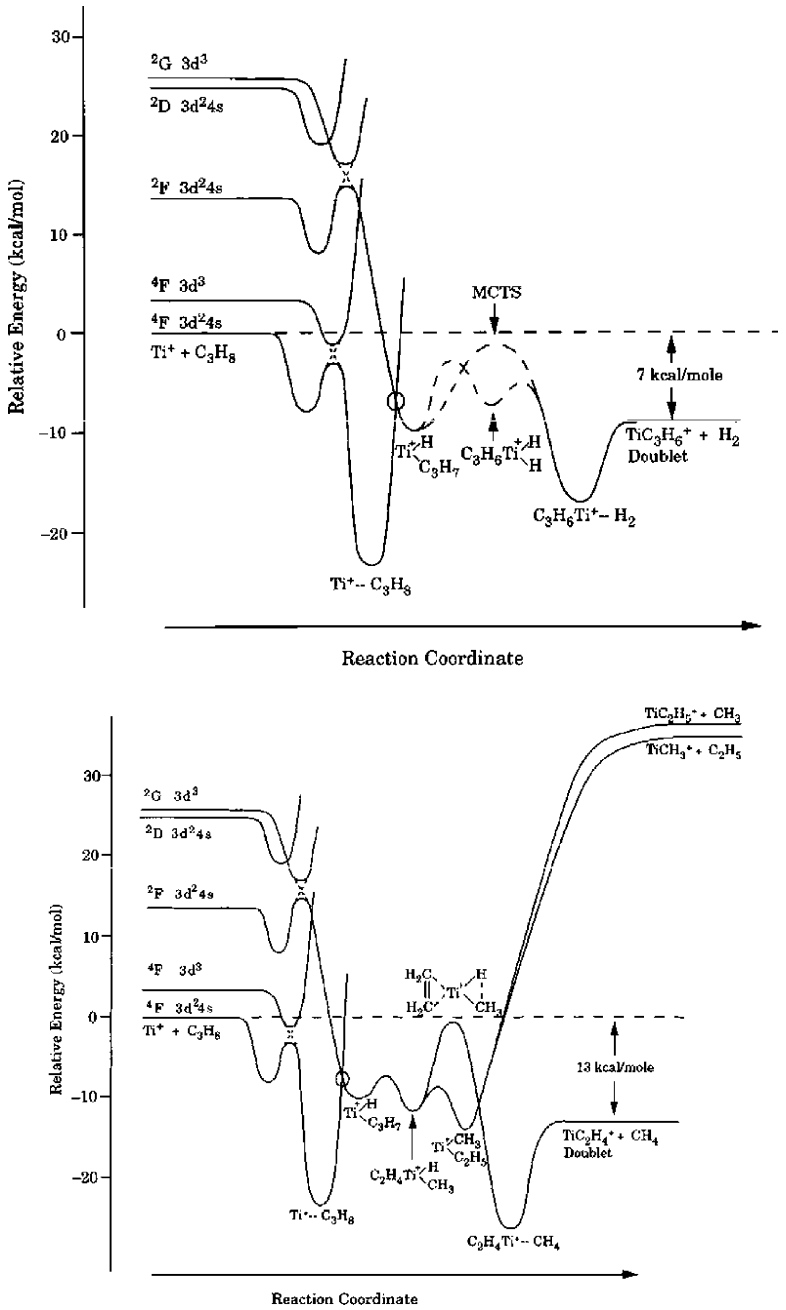

Fig. 9. Schematic reaction profiles for the reactions of Ti^+ with C_3H_8 to eliminate (a, top) H_2 and (b, bottom) CH_4. MCTS stands for multi-centre transition states; for details, see Ref. [82]. Reproduced from *J. Am. Chem. Soc*. 120 (1998) 5704.

confirmed by electronic structure calculations for $Cr(CH_3)_2^+$ [85]; thus, C−C and C−H bond activation is spin-forbidden from the sextet states of Cr^+ and spin-allowed from the quartet states. Differences in reactivity between these different states can thus be readily explained. Further, while the initial interaction between all states of Cr^+ and the alkanes is attractive due to long-range ion-induced dipole forces, at closer distances the surfaces arising from the ^6D and ^4D terms become fairly repulsive due to the 4s occupations; in contrast, those states with empty 4s orbitals, i.e., ^6S and ^4G, evolve into surfaces that are less repulsive. The ^4G state is the lowest state of Cr^+ having both the correct spin and electron configuration to correlate directly to the ground states of the insertion intermediates. Since the two quartet surfaces ^4D and ^4G cross one another and are close in energy, they are likely to mix and thereby allow the ^4D state to also react efficiently. The branching ratios of the C−H versus C−C bonds is by and large the result of differences in Cr^+−H versus Cr^+−C bond strength favouring the latter one.

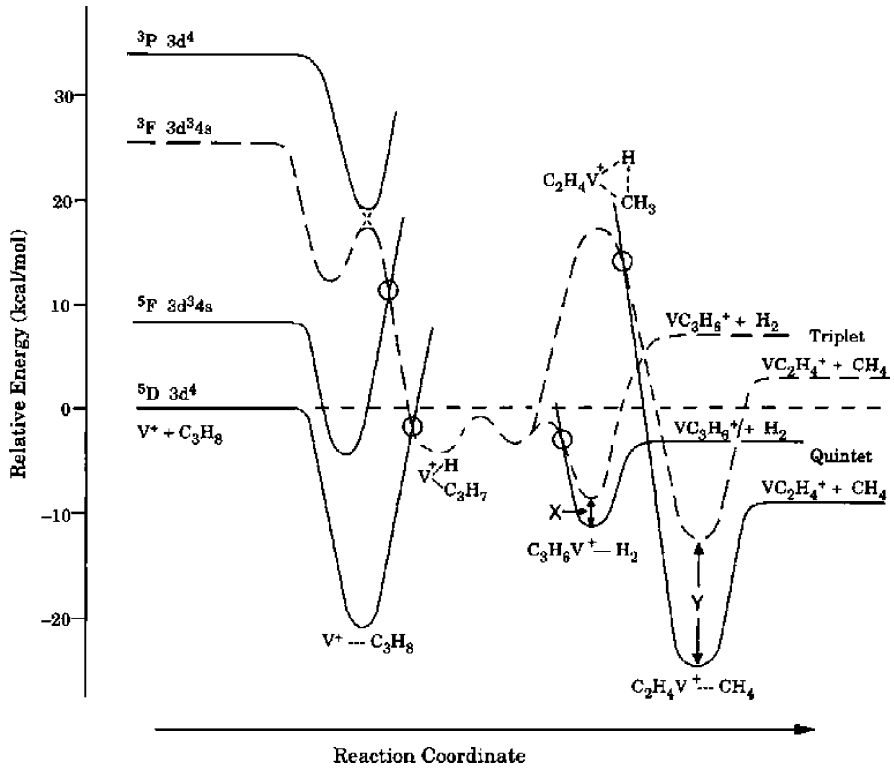

Fig. 10. Schematic reaction profile for the reaction of V^+ with C_3H_8 to eliminate H_2 and CH_4. Triplet surfaces are dashed, and quintet surfaces are solid lines. *X* and *Y* correspond to the energies of the triplet−quintet splitting for $(C_3H_6)VH_2^+$ and $(C_2H_4)VCH_4^+$, respectively. Reproduced from *J. Am. Chem. Soc*. 120 (1998) 5704.

3.5. Activation of NH and H_2O by atomic metal ions—still more to learn

Activation of N−H bonds is of topical interest. In the gas phase, *exothermic* dehydrogenation of NH_3 by ground-state atomic metal ions M^+, Eq. (28), is confined to group 3, 4, and 5 transition metals. They react at thermal energies to generate MNH^+ [86] which implies $D(M^+-NH) > 101$ kcal/mol [87,88]. Atomic metal ions from group 6–11 undergo slow condensation to form MNH_3^+ adducts [86],

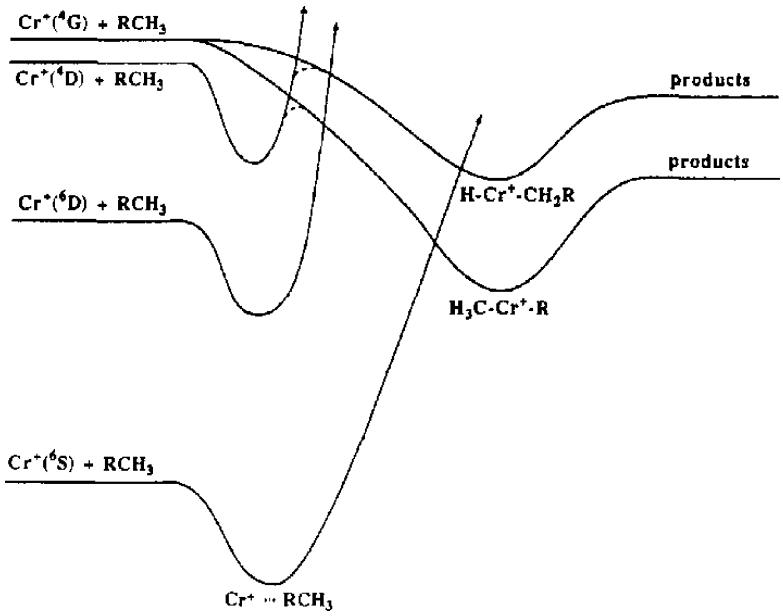

Fig. 11. Qualitative generalized energy curves for the reactions of Cr^+ with alkanes RCH_3. Reproduced from *J. Am. Chem. Soc*. 114 (1992) 2049.

and for these 'late' transition metals dehydrogenation is endothermic.

$$M^+ + NH_3 \rightarrow MNH^+ + H_2 \quad (28)$$

The electronic and translational energy dependence of NH_3 dehydrogenation was studied for M = V in a guided ion beam experiment [87], and the results indicate that the most likely reaction mechanism proceeds via oxidative addition of a N−H bond to yield $H-V^+-NH_2$. Simple bond cleavage forms VH^+ and $VNH_2{}^+$ in endothermic processes, producing preferentially the former one due to better conservation of orbital angular momentum. Exothermic formation of VNH^+ occurs via four-centre elimination of molecular hydrogen. The a^3F state of V^+ is found to be substantially more reactive than the a^5D ground and a a^5F first excited state even after accounting for differences in available energy. These reactivity dependences on electronic states have been explained by using the same concepts as outlined above for the reactions of early transition-metal cations with CH_4, and the much higher reactivity of the triplet state reflects spin-allowed oxidative insertion of V^+ in the N−H bond coupled with a favourable thermochemistry. In contrast, all reactions emerging from quintet states are spin-forbidden, and the poor efficiency suggests rather small spin–orbit coupling for this particular system.

More refined theoretical studies on several aspects of the metal-mediated ammonia activation have been performed for M^+ = Sc^+ [70,89], Fe^+ [65] and Ni^+, Cu^+ [89], and some features will be presented next. For the Sc^+/NH_3 system a picture emerges which substantiates what has been described above for the related V^+/NH_3 reactions. In particular, spin–orbit mediated crossing between the triplet and singlet surfaces is essential and occurs *after* formation of the $ScNH_3{}^+$ encounter complex (Fig. 12) [70]; the reaction proceeds then adiabatically on this surface towards $ScNH^+/H_2$ [70,89] with $H-Sc^+-NH_2$ serving as intermediate [90].

The experimentally observed differences in the behaviour of 'early' versus 'late' 3d cations M^+ with regard to dehydrogenation of NH_3, Eq. (28), are also born out by theoretical studies [65,89], and brief mentioning of four aspects obtained for the Fe^+/NH_3 system [65] may suffice: (1) Dehydrogenation of NH_3 by Fe^+ is very endothermic and thus will not occur under thermal conditions [86]. (2) The association complex $FeNH_3{}^+$ corresponds to a quartet state with a calculated binding energy of 46.6 kcal/mol, relative to the $Fe^+(^6D)$ ground state, in excellent agreement with the experimental value of 46.7 kcal/mol [91]. Surface crossing between the sextet and quartet manifolds occurs close to the entrance channel of the reaction. (3) If insertion of Fe^+ into the N−H bond, to generate $H-Fe^+-NH_2$, proceeds on the quartet surface, the corresponding transition structure is energetically located below the entrance asymptote, contrary to the behaviour of the sextet $FeNH_3{}^+$ complex. (4) In distinct contrast to 'early' transition-metal cations, e.g., Sc^+, the rate limiting step in the dehydrogenation of NH_3 corresponds in the Fe^+/NH_3 system to the four-centre-transition state to generate $Fe(NH)(H_2)^+$, in which H_2 is only weakly interacting with the $FeNH^+$ core.

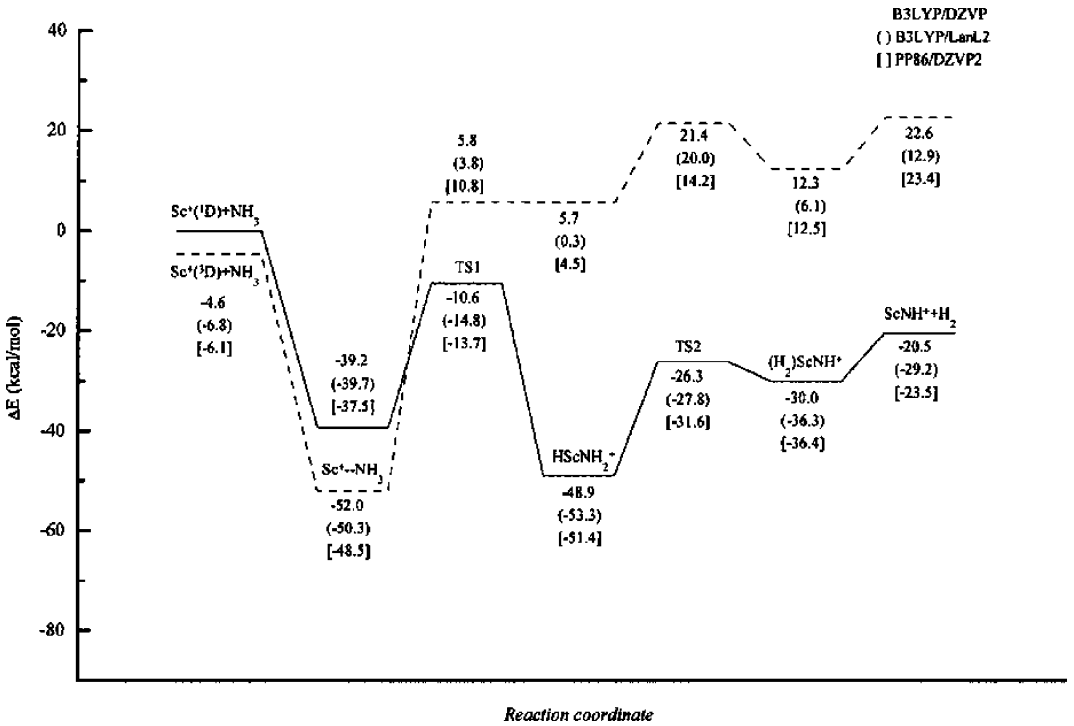

Fig. 12. B3LYP/DZVP singlet and triplet potential energy surfaces for the reactions of $Sc^+(^1D, ^3D)$ with NH_3. Reproduced from *J. Am. Chem. Soc.* 123 (2001) 2588.

Dehydrogenation of H_2O by M^+, Eq. (29), constitutes the reversal of H_2-oxidation by diatomic metal oxides, and as Chapter 4 is reserved to describe in detail various aspects of this metal oxide mediated process, the many experimental and theoretical studies reported on reaction (29) will be discussed here only briefly.

$$M^+ + H_2O \rightarrow MO^+ + H_2 \quad (29)$$

The 'early' transition-metal ions Sc^+, Ti^+ and V^+ react exothermically with water, and in line with the related M^+/NH_3 system, for all three metals the low-spin excited states react more efficiently than the high-spin ground states [88,92]. This is indicative for the formation of a low-spin insertion intermediate $H-M^+-OH$. Mechanistic details of reaction (29), as derived from extensive theoretical studies, are in many ways surprisingly similar to the profile shown in Fig. 12 for dehydrogenation of NH_3 by M^+, and in-depth computational analyses for the M^+/H_2O couples exist for Sc^+ [3h,70,93,94], Ti^+ [95], and V^+ [94]. Here, only the Sc^+/H_2O system will be presented. Common to all computational studies is that key stationary points on the singlet and triplet PESs had been characterized, and these include the ScH_2O^+ association complex, the transition state (TS) leading to the intermediate $H-Sc^+-OH$, the H_2 elimination TS, and the resulting ScO^+-H_2 ion–molecule complex, with the latter three points all having singlet ground states. The effect of spin on this reaction has only loosely been discussed, and Irigoras et al. [94] claimed that the singlet PES crosses below the triplet one somewhere between the reactant complex ScH_2O^+ and the insertion intermediate $HScOH^+$, at an energy below the entrance channel. In a more recent study using a procedure for localizing minimum energy crossing points MECPs [18], the issue of the crossing behaviour has been analyzed more rigorously (J.N. Harvey, unpublished results mentioned in [3h]); the results are depicted in Fig. 13. The MECP is indeed found to be lower in energy than the Sc^+/H_2O asymptote, and very close, both in geometry and in energy, to the TS that separates $^3ScH_2O^+$ and $^1HScOH^+$ located on the $^3A'$ and $^1A'$ PESs. However, the actual triplet → singlet crossing occurs *after* passing the TS on the triplet surface.

Both state-specific reactions [96] of $Fe^+(a^6D, a^4F)$ and extensive calculations [65,97] have been employed in the hope to unravel at least a few of the many intriguing features of the Fe^+/H_2O system, the detailed discussion of which will be postponed to Chapter 4.

For the late transition-metal oxides M^+ (M = Cr, Mn, Fe, Co, Ni, and Cu), reaction (29) is endothermic. Some mechanistic aspects of both high- and low-spin components of these metal ions were uncovered by computational studies [97,98]; for example, an increase in endothermicity exists through the 3d metal series from the left to the right. Fe^+ is significantly different from the entire Sc^+-Mn^+ series because both its low- and high-spin terms involve paired electrons and both states are engaged in the reaction ('two-state reactivity' behaviour [3g]), and Mn^+ exhibits some deviations because of the complete half-filling of its valence shell in the high spin. What is, however, quite unsatisfying is the lack of precise information on the exact location of the MECPs as well as on the efficiency of spin–orbit coupling, which, admittedly, is all but trivial to obtain given the enormous electronic complexity of these deceptively trivial molecules.

3.6. Activation of double bonds in X=C=Y by atomic M^+

Systems being studied in detail in the gas phase include the following couples: V^+/CS_2 [99], V^+/CO_2 [100,101],

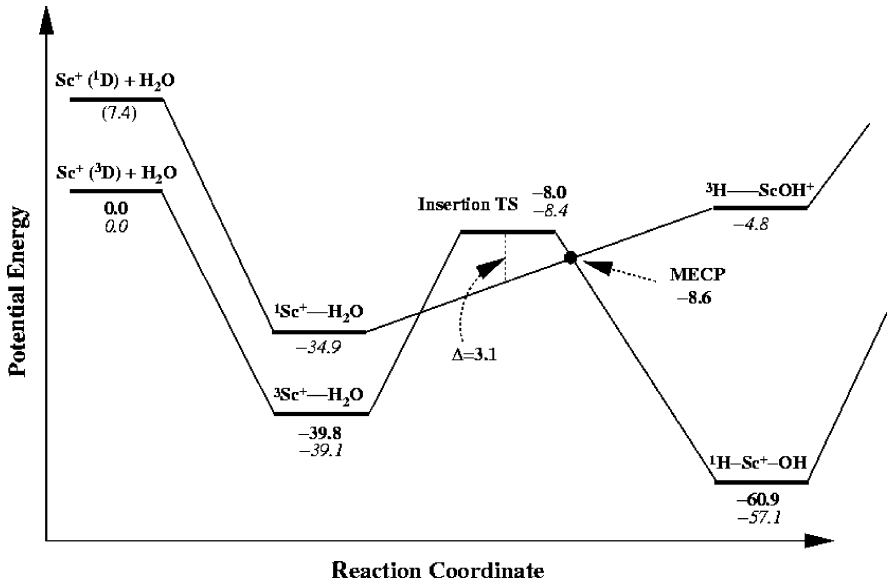

Fig. 13. Simplified potential energy curves for $Sc^+(^1D, ^3D)$ and H_2O. Energies are in kcal/mol relative to reactants, with the numbers in bold taken from Ref. [94] and the numbers in italics from Ref. [3h]. The excitation energy of Sc^+ is the experimental value. For further computational details, see Ref. [3h]. Reproduced from Ref. [3h].

V^+/COS [101], Cr^+/CS_2 [102], Cr^+/COS [102], Mn^+/CS_2 [102], Mn^+/COS [102], Fe^+/CS_2 [103a], Fe^+/COS [103a], Co^+/CS_2 103a], Co^+/COS [103a], Sc^+/COS [103b], Sc^+/CS_2 [103b], Ti^+/COS [103b], Ti/CS_2 [103b], and Ni^+, Cu^+ and Zn^+ reacting with COS and CS_2, respectively [103c]. For all these examples, two-state reactivity (TSR) has been either proven or implied to play a decisive role in the bond activation step.

The by far most convincing study concerns an intriguing situation which was found for the endothermic sulfur atom transfer from CS_2 to atomic V^+, Eq. (30). This process is a textbook example for the operation of TSR and, therefore, deserves special mentioning.

$$V^+ + CS_2 \rightarrow VS^+ + CS \quad (30)$$

The kinetic-energy dependence of this, as we shall see, competitive spin-allowed and spin-forbidden, reaction was examined using guided ion beam mass spectrometry, and by systematically varying the V^+ electronic state distributions, the reactivities of both the ground and excited state of V^+ were determined. Extensive DFT calculations and determinations of the Landau–Zener surface crossing probabilities were instrumental in obtaining a quite comprehensive picture of this elementary chemical transformation [99].

The bimodal kinetic energy dependence of reaction (30) observed in the low-energy part of the VS^+ cross-section, Fig. 14, is very unusual. The first endothermic feature corresponds to the formation of ground state VS^+. This process has an apparent threshold near 0.4 eV, peaks around 1.2 eV, and falls to ca. two-thirds of its maximum intensity before the rise of a second endothermic feature near 2.3 eV. Because no products other than VS^+ and CS are feasible in this energy regime [101], the second feature must correspond to the formation of electronically excited VS^+. Electronic excitation of the CS neutral product can be ruled out. Clearly, the routes to the two cationic products in question must differ in some fundamental way. Electronic structure calculations [101] predict

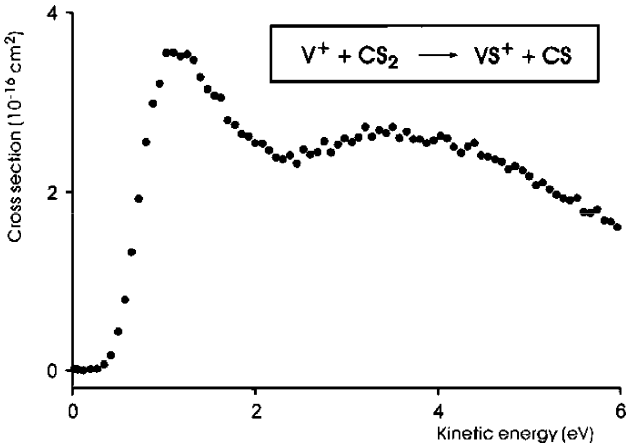

Fig. 14. Cross-section for the formation of VS^+ in the reaction of V^+ with CS_2 as a function of centre-of-mass energy (for details, see Ref. [100]). Reproduced from *Acc. Chem. Res.* 33 (2000) 139.

a $^3\Sigma^-$ ground state for VS^+ with the first quintet state ($^3\Pi$) lying 1.37 eV higher in energy. Thus, the formation of ground state products from ground-state reactants is spin-forbidden, Eq. (31a) while at higher energies the spin-allowed production of excited VS^+ can occur, Eq. (31b).

$$V^+(^5D) + CS_2(^1\Sigma_g^+) \rightarrow VS^+(^3\Sigma^-) + CS(^1\Sigma^+) \quad (31a)$$

$$V^+(^5D) + CS_2(^1\Sigma_g^+) \rightarrow VS^+(^5\Pi^-) + CS(^1\Sigma^+) \quad (31b)$$

The calculated energy difference of 1.37 eV between the two VS^+ states in question is in good agreement with the observed threshold difference of 1.45 eV between the two features in Fig. 14. The distinct fall and secondary rise of the cross-sections are consequences of the spin-forbidden character of reaction (31a), which leads to the decline above 1.2 eV, combined with an enhanced reaction efficiency once the spin-allowed process (31b) is energetically accessible.

Further insight about the surface-crossing behaviour is provided by the computed potential energy surfaces for processes (31a) and (31b), Fig. 15 [99], together with a Landau–Zener analysis [104] of the cross-section.

As expected, the VCS_2^+ encounter complex **1** has a $^5A''$ ground state correlating with $V^+(^5D)$ + CS_2 reactants. However, coordination of CS_2 to V^+ significantly lowers the triplet surface compared to atomic V^+, and **1**($^3A''$) is predicted to be 0.67 eV below the ground-state entrance channel. For the product complexes $SVCS^+$ (**2**) the order of stability is reversed, and the differences between the $^3A''$ and $^5A''$ states simply reflect the relative stabilities of the respective fragmentation channels. Thus, for the V^+/CS_2 system, the lowest-energy adiabatic surface is quintet-like in the reactant region and triplet-like in the product region, and spin-inversion must occur en route to products. While the MECP for this event has not been explicitly located, indirect arguments have been developed [99] to position this point between the closely spaced **1** ($^3A''$) and TS**1/2** ($^3A''$) species with an estimated spin–orbit coupling constant of 20 cm^{-1}; this value lies in the weak-coupling limit [105].

Equipped with these information (and additional considerations [99]) the explanation of the bimodal cross-section of Fig. 14 is straightforward. At low kinetic energies, the reactants pass slowly through the crossing region, allowing the electrons to adjust to different configurations along the reaction coordinate. Under such conditions, spin inversion can take place, and adiabatic behaviour is expected. As the nuclear motion speeds up at elevated kinetic energies, the reactants pass more quickly through the crossing region, the electrons have less time to adapt, and the Born–Oppenheimer approximation begins to fail. Thus, it becomes increasingly likely that the reactants will stay on their initial surface and behave diabatically, and the enhanced probability for spin-conserving behaviour appears to be responsible for the premature decline of the first feature associated with the formally spin-forbidden reaction (31a). Consequently, the VS^+ cross-section decreases from the maximum near

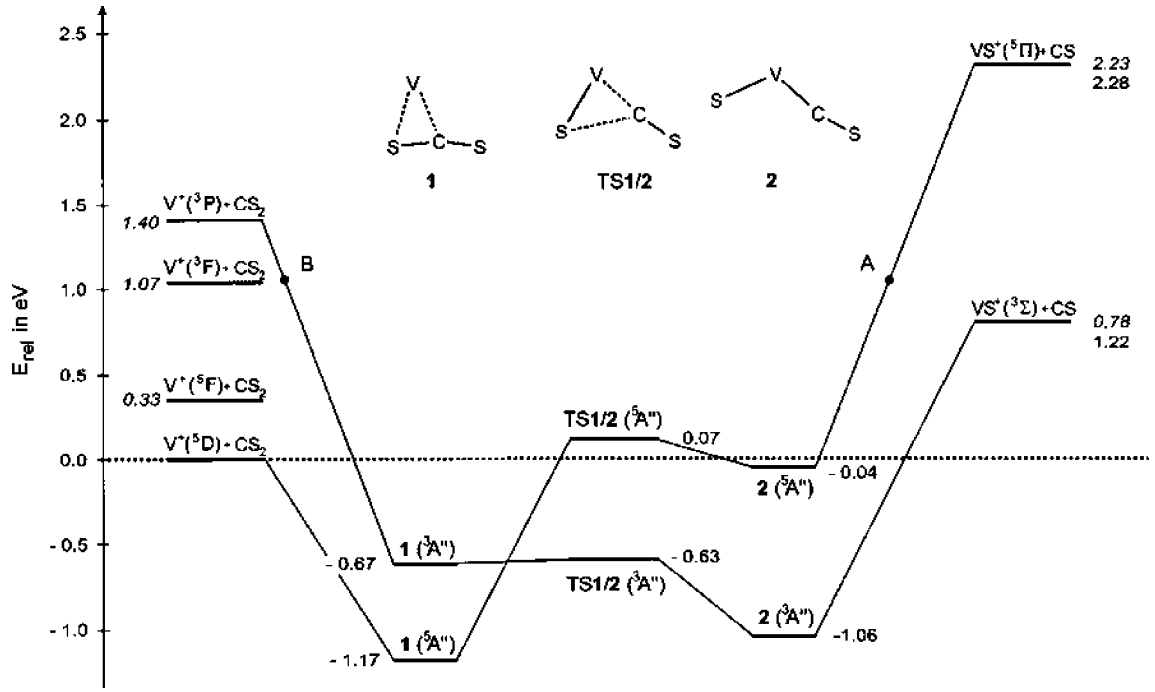

Fig. 15. Potential energy curves for the V^+/CS_2 system calculated at the B3LYP/6-311 + G* level of theory. Energies are given in eV, and experimental energies for the reactant and product asymptotes are given in italics. Reproduced from *J. Chem. Phys.* 110 (1999) 7858.

1.2 eV until diabatic formation of the excited quintet state $VS^+(^5\Pi)$ is energetically feasible near 2 eV.

4. The gas-phase world of cationic metal oxides

4.1. General remarks

The enormous interest in the chemistry of transition-metal oxides (and also sulfides) evolves primarily from their numerous applications, e.g., as catalysts, lubricants, support materials, or superconductors, to mention only a few [106]. Moreover, transition-metal chalcogenides are found in the reaction centres of many enzymes [107], and metal sulfides have even been postulated to be essential for the evolution of life [108]. Also the gas-phase chemistry of small charged metal chalcogenides has been studied in great detail, both experimentally and computationally. For example, the fascinating binding situation in neutral and cationic 3d and 4d $MX^{0/+}$ species (X = O, S) has been summarized by Kretzschmar et al. [109]. A categorization and the characterization of orbital descriptions, as well as the analysis of reactivity pattern of transition-metal oxides form the theme of a review by Schröder et al. [110], and a comprehensive collection and an in-depth discussion of the electronic structure of metal oxides can be found in an exhaustive review of Harrison [43]. Further, the analysis of the electronic structure constitutes the subject of an early theoretical investigation by Carter and Goddard [111]. In this latter study, fundamental differences in the nature of the metal-oxo bond in 'early' and 'late' metal-oxo complexes were described that were used to explain observed trends in reactivity. Finally, an overview on C−H and C−C bond activation by gaseous metal-oxide cations, summarizing the then known experimental work, was published in 1995 by Schröder and Schwarz [112].

In the following the focus will be on the reactions of binary MO^+ with molecular hydrogen and small hydrocarbons, Eq. (32), with an emphasis on those systems in which two-state reactivity patterns are crucial.

$$MO^+ + RH \rightarrow M^+ + ROH\,(R = H,\ alkyl) \qquad (32)$$

Note, that reaction (32) is the reversal of ROH deoxygenation by bare M^+, Eq. (29), which has been analyzed in Chapter 3.5. Some of the arguments already presented there, in particular those for the couples M^+/H_2O and M^+/CH_4, respectively [65,96–98], hold true for reaction (32) as well and, therefore, will not be repeated here in detail.

Generally speaking, comparative studies of M^+/MO^+ with RH (R = H, CH_3) often reveal an inverse reactivity pattern: For highly reactive metal ions M^+ their corresponding metal oxides react sluggishly and vice versa, and the couple Mn^+/MnO^+ represents perhaps an extreme example: Mn^+ is the least reactive 3d transition-metal cation toward alkanes, whereas MnO^+ is the most reactive one [113]. Further, as has been repeatedly suggested [109–112,114], the overall reactivity of the MO^+ species seems to inversely correlate with its stability. For example, for the metal oxides CrO^+ [114], MnO^+ [113,115], FeO^+ [55,116] and OsO^+ [61a] it has been shown that the oxo ligand increases the reactivity of the bare metal. However, for systems involving the 'early' metals Sc^+ [117,119], V^+ [118,119], and Ti^+ [119], oxida-

tion of these metals to MO^+ suppresses the reactivity relative to M^+ [112].

Finally, Chapter 4 will close with brief mentioning of some aspects relevant for an understanding of the formation and the reactivity of a few metal dioxides to the extent that their chemistry is TSR-controlled.

4.2. Oxidation of molecular hydrogen

For the 'early' metal oxides ScO^+, TiO^+, and VO^+, cross-section measurements in a guided ion beam experiment demonstrate that for all three MO^+ cations their reactions with D_2 to form M^+ and D_2O are *endothermic* [119], and M^+ are primarily formed in an excited low-spin electronic state. Production of ground-state M^+ is also observed via spin crossing from a low-spin to a high-spin surface, exactly in analogy to the reverse reaction depicted in Fig. 13. The inefficiency of forming the ground-state metal ions in these systems indicates a rather poor spin–orbit coupling. Further, this model can rationalize why the amount of M^+ produced decreases from the Sc^+ to the Ti^+ to the V^+ system. Because the energy splittings between the high- and low-spin M^+ states increase from Sc^+ (0.3 eV) to Ti^+ (0.6 eV) to V^+ (1.1 eV), the coupling efficiency between the reaction surfaces evolving from these states decreases and the cross-section of M^+ formed gets smaller.

One of the best studied couples, both experimentally and computationally, concerns the oxidation of H_2 (and its isotopologues HD and D_2) by diatomic FeO^+, Eq. (33) [96,120–126].

$$FeO^+(^6\Sigma^+) + H_2 \rightarrow Fe^+(^6D) + H_2O \quad (33)$$

This reaction is very exothermic ($\Delta_r H^0 = -37$ kcal/mol), even so when excited $Fe^+(^4F)$ is formed, orbitally unrestricted, and spin-allowed—and yet the reaction efficiency is <1% [124]. Further features of the molecular hydrogen oxidation by FeO^+ are the very small intra- and intermolecular kinetic isotope effects on the reaction efficiencies for H_2, HD, and D_2 [121,123]. The most intriguing finding is that in the vicinity of the threshold the cross-section of reaction (33) (with D_2 being used in order to enhance mass resolution in the GIB experiment [124]) slightly *diminishes* with increasing energy (Fig. 16).

While the small reaction efficiency (<1%) could be interpreted in terms of a classical Arrhenius activation barrier [123], this assumption perhaps does not seem justified in view of the results of the guided ion beam experiment which shows that the cross-section monotonically decreases with increasing collision energy below 0.2 eV (Fig. 16). Hence, the vanishingly low reactivity of FeO^+ toward molecular hydrogen may well be related to the inefficiency associated with switches between surfaces of different spin. This scenario is in line with extensive computational studies conducted by Shaik and coworkers [120,122,125,126].

In a comprehensive computational undertaking [126,127], various mechanistic variants for reaction (33) were considered, and based on a comparison with the experimental findings, the potential energy profile depicted in Fig. 17 [125] emerged as the most likely scenario—obviously, this is yet another prototype of two-state reactivity for a *thermal* reaction [122].

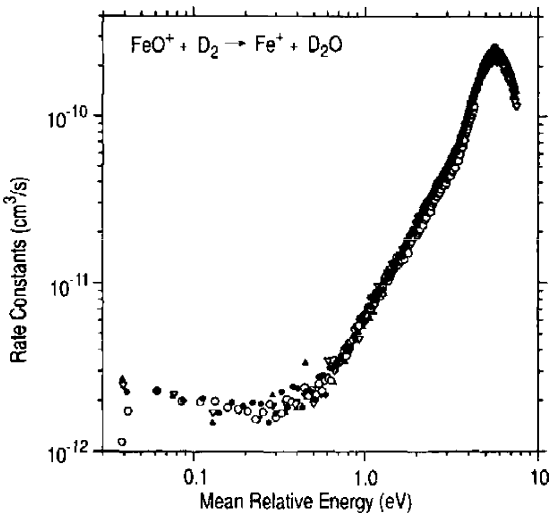

Fig. 16. Guided ion beam (GIB) results for the variation of the rate constant for the reaction of FeO^+ with D_2 to form Fe^+ and D_2O as a function of kinetic energy in the centre-of-mass frame. Reproduced from *Int. J. Mass Spectrom. Ion Process.* 161 (1997) 175.

The process involves two spin inversion (SI) junctions between sextet and quartet states, one near the FeO^+/H_2 cluster at the entrance channel and one near the Fe^+/H_2O complex at the exit channel. Spin–orbit coupling calculations indicate a continuous decrease of the SOC value from being significant at the entrance to become negligibly small at the product exit. The results further show that while the quartet surface provides a low-energy path, the SI junctions reduce the probability of the reaction significantly, and the suggested interplay between spin inversion and chemical barrier height in the FeO^+-mediated oxidation of molecular hydrogen is confirmed by the pleasing agreement of the experimentally determined kinetic isotope effects of reaction (33) (with HD and D_2) with the computed data [126]. Finally, quite clearly without the intervention of spin inversion at thermal condition, reaction (33), should *not* take place at all, and the observation of it, though being quite inefficient, is a convincing example for the concept of a 'spin-accelerated reaction' [3k], the essence of which is sketched in Fig. 18.

It is not without irony (or satisfaction, depending on one's view point) to recall, that the gas-phase studies of one of the smallest molecular systems conceivable, i.e., the four-atomic FeO^+/H_2 couple, have paved the way to resolve some of the puzzling questions associated with the mechanisms by which the enzyme cytochrome P-450 brings about oxygenation of a C−H bond [3i,31,128,129]. Aspects of the timely topic of C−H bond oxygenation will be addressed in the next chapter, and we shall see that the two-state reactivity concept serves well as a guiding principle.

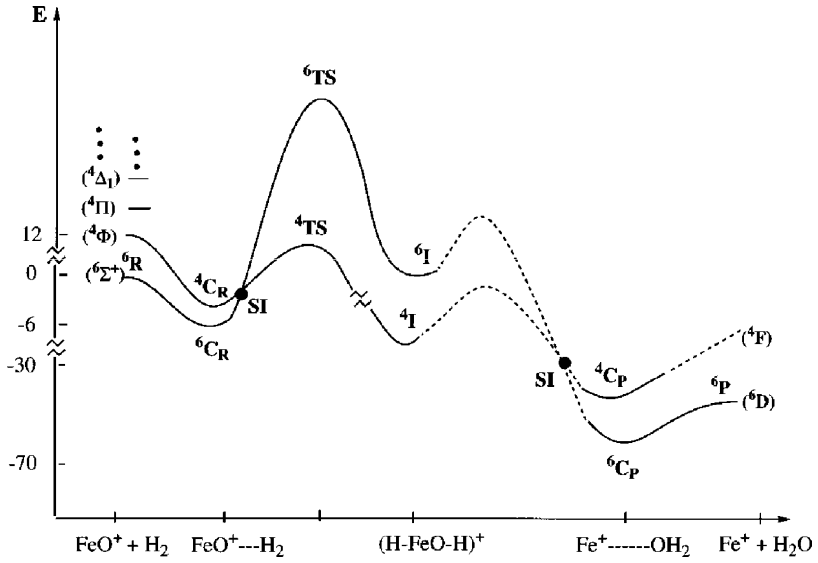

Fig. 17. Schematic potential energy profile for reaction (33). Relative energies are given in kcal/mol. The dashed lines indicate areas unexplored computationally. Some energies were taken from Refs. [121,128]. The meaning of the abbreviation employed is as follows: C_R reactant complex; SI spin inversion; I insertion intermediate; and C_P product complex. Reproduced from *J. Am. Chem. Soc*. 119 (1997) 1773.

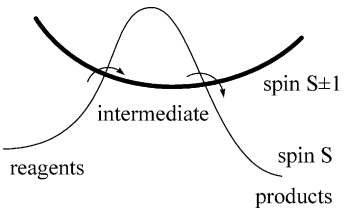

Fig. 18. Qualitative energy profile for a spin-accelerated reaction. Reproduced from *Chem. Soc. Rev*. 32 (2003) 1.

4.3. Oxygenation of C−H bonds by MO^+: a "holy grail in chemistry"

Relating Sir Derek Barton's famous dictum about "Holy Grails in Chemistry" (A whole issue of the *Accounts of Chemical Research* has been devoted to this topic) [130,131] to the oxygenation of C−H bonds in alkanes, Eq. (34), is not unjustified given the challenging complexity of this deceptively trivial reaction which only on paper looks so easy [132].

$$R - H + \langle O \rangle \rightarrow ROH \quad (34)$$

In the reactions of diatomic MO^+ with CH_4, three principal product channels are conceivable, Eq. (35), the efficiencies and branching ratios of which are controlled by thermochemical and spin considerations. It should be mentioned, that reaction (35c) is unimportant for 3d metal oxides, in contrast to 5d metal oxides [113].

$$MO^+ + CH_4 \rightarrow M^+ + CH_3OH \quad (35a)$$
$$\rightarrow MOH^+ + CH_3 \quad (35b)$$
$$\rightarrow MCH_2^+ + H_2O \quad (35c)$$

The most detailed study, both in regard to experimental and computational efforts, has been conduced for FeO^+ reflecting the particular role this metal plays in oxidation chemistry in general [106b,107,132,133]. Rate constants and branching ratios, obtained by using three different mass spectrometric methods, are reported in Table 1, and a thorough discussion of the experimental findings can be found in Ref. [124].

As described above for the related FeO^+/H_2 system (Fig. 16), the most intriguing experimental observation is the rate constants dependence for the FeO^+/CH_4 reaction, Fig. 19 [124], as a function of kinetic energy.

Similar to reaction (33), at very low kinetic energy the efficiencies for the formation of $FeOH^+$ and Fe^+ from CH_4 *decrease* with *increasing* energy, thus displaying a significant kinetic bottleneck in a reaction which is exothermic for channel 35a (M = Fe) and thermoneutral for process (35b) (M = Fe). As in the case of the FeO^+/H_2 couple, the unusual behaviour of FeO^+/CH_4 can be traced back to the existence of a spin barrier in the crossing from the sextet to a quartet surface close to the entrance channel. This picture has been corroborated by extensive potential energy surface calculations, including an analysis of the relevant spin–orbit coupling terms [120,122,125,134]. In Fig. 20 a potential energy

Table 1
Rate constants k (in 10^{-11} cm^3 s^{-1}) for the reactions of FeO^+ with methane and branching ratios between Fe^+ and $FeOH^+$ in the ICR, GIB, and SIFT experiments

Method	k	Fe^+:$FeOH^+$
ICR	8.5 ± 2.6	39:61
GIB	2.8 ± 0.8	29:71
SIFT	7.4 ± 2.2	81:19

ICR: ion cyclotron resonance, GIB: guided ion beam, and SIFT: selected ion flow tube. Only in the ICR experiment, the product $FeCH_2^+$ is formed with very small abundance (<1%).

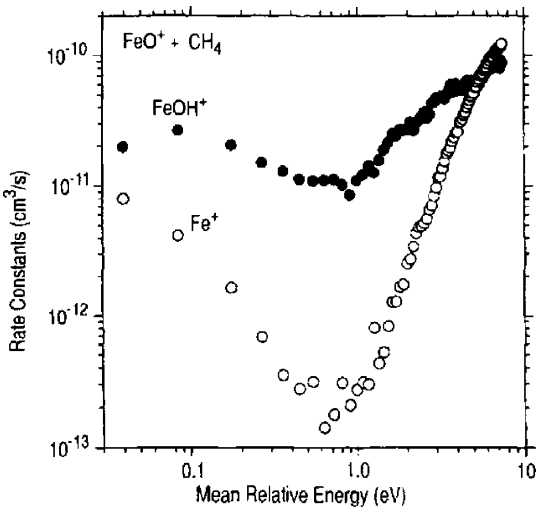

Fig. 19. GIB results for the variation of the rate constants, k_{CH_4}, for the reaction of FeO^+ with CH_4 to form $FeOH^+ + CH_3$ (closed circles) and $Fe^+ + CH_3OH$ (open circles) as a function of kinetic energy in the centre-of-mass-frame. Reproduced from *Int. J. Mass Spectrom. Ion Process.* 161 (1997) 175.

diagram, taken from one of the more recent theoretical studies [134e], is given.

From the three crossing points calculated, the one between the encounter complex $(CH_4)FeO^+$ and the transition state towards the quartet intermediate $H_3C{-}Fe{-}OH^+$ exhibits the largest spin–orbit coupling element (133.6 cm^{-1}), the energetically feasible interconversion between the sextet and quartet states of the insertion intermediate has an SOC of 21.4 cm^{-1}, and the one at the exit channel is the smallest with 0.3 cm^{-1} only. Provided the crossing points reported in Fig. 20 correspond to the true minimum energy crossing points and the respective SOC calculations are reliable, one arrives at the conclusion that in the experimentally demonstrated formation of Fe^+ in its ^6D ground state [124], the rate-limiting step in the multi-sequence event corresponds to the quartet → sextet spin inversion at the exit channel, and not the one close to the entrance as argued in Ref. [134e]. Alternatively, the system changes back from the quartet to the sextet state at the stage of the insertion intermediate $H_3C{-}Fe{-}OH^+$, and will then proceed adiabatically at the sextet surface via TS2 towards $Fe^+(^6D)$ and CH_3OH.

Computational studies of all 5d-metal-oxide cations $ScO^+{-}CuO^+$ and their role in the methane–methanol conversion have been performed by Shiota and Yoshizawa [134d], and these exhaustive computations are quite revealing concerning mechanistic details, reaction efficiencies as well as product ratios depending on the nature and the electronic structure of the diatomic metal oxide. Before briefly addressing these theoretical findings [113,134d] it is appropriate to summarize the experimental data obtained under ICR conditions for M = Mn, Fe, Co, and Ni in reactions of their metal oxides MO^+ with CH_4, Eq. (35a) and (35b). The relevant data are given in Table 2 and taken from Refs. [112,124].

The high efficiency, defined according to Su [135], and the product selectivity for the MnO^+/CH_4 couple can be easily explained in terms of the potential energy surface [134d] and spin considerations [113,122,125]. $MnO^+(^5\Sigma^+,^5\Pi)$ undergoes a spin-conserving bond insertion via a transition-state located below the entrance channel to form the quintet insertion intermediate $H_3C{-}Mn{-}OH^+$, but had to cross a spin-inversion junction with a small SOC value at the exit channel to produce $Mn(^7S)$ and CH_3OH. This bottleneck is bypassed by the spin-allowed, barrier-free and entropically favoured dissociation of the insertion intermediate to yield

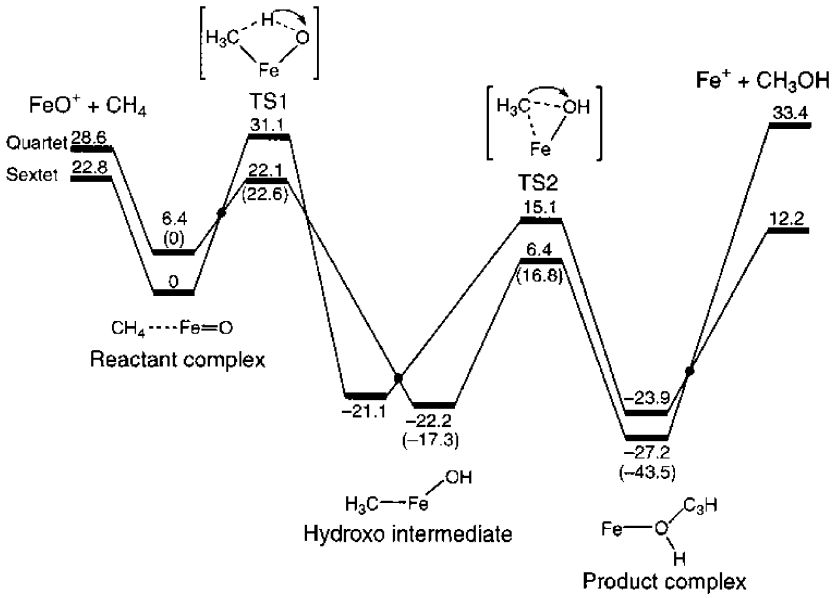

Fig. 20. DFT-calculated potential energy curves along the reaction pathways $FeO^+ + CH_4 \rightarrow FeO^+ + CH_3OH$ in the quartet and sextet states. Relative energies are given in kcal/mol; values in parentheses are results obtained at the CASSCF level. The closed circles indicate crossing points along the crossing seams. Reproduced from *J. Chem. Phys*. 118 (2003) 5872.

Table 2
Reaction efficiencies (ø) and relative yields for the reactions of MO^+ with CH_4 under ICR conditions

MO^+	ϕ[a]	M^+/CH_3OH	MOH^+/CH_3
MnO^+	0.40	<1	100
FeO^+	0.20	39	61
CoO^+	<0.01	100	–
NiO^+	0.20	100	–

[a] $\phi = k_r/k_c$, with k_c = collision rate [136].

$MnOH^+/CH_3$. In contrast, CoO^+ and NiO^+, which possess a SI junction for bond insertion, do not have to invert spin at the elimination step because the ground state of the corresponding metal ion is of $3d^n$ configuration. While both metal oxides undergo good to inefficient bond activation, the differences in efficiency are being caused by details of the individual barrier for the insertion-step and also presumably different SOC terms, they nevertheless produce exclusively M^+/CH_3OH. The behaviour of FeO^+ is in-between, and as indicated by the computational studies, it is the most difficult of all 3d metal oxides to be described quantitatively in its bond activation reactions.

Before presenting some TSR cases for metal dioxides MO_2^+, a short detour to the chemistry of FeS^+ with methane is in order at this place, as this cationic metal sulfide can be regarded as the smallest conceivable model system for mimic larger iron–sulfur clusters [136].

In the endothermic hydrodesulfurization of FeS^+ by molecular hydrogen, ICR and GIB experiments, complemented by electronic structure calculations, demonstrated a predominance of kinetic over thermodynamic control [137]. The lowest energy path for Fe−S bond activation involves [1.2]-addition of hydrogen across the Fe−S bond along with two spin inversions. The first one occurs close to the entrance channel and describes the sextet → quartet change in converting the encounter complex to the insertion intermediate, and the second one is located at the exit channel in producing ground-state Fe^+. Thus, while the overall reaction, Eq. (36), conserves spin, as far as details are concerned, spin changes do matter en route to products and bring about an overall rate-acceleration.

$$FeS^+(^6\Sigma) + H_2 \rightarrow Fe^+(^6D) + H_2S \quad (36)$$

Except for thermochemical aspects, methane to methanethiol conversion by FeS^+, Eq. (37a), has many features in common with the oxygenation of methane, discussed above.

$$FeS^+ + CH_4 \rightarrow \begin{cases} Fe^+ + CH_3SH & (37a) \\ FeSH^+ + CH_3 & (37b) \\ FeSCH_3^+ + H & (37c) \\ FeCH_3^+ + SH & (37d) \end{cases}$$

In the reaction of FeS^+ with D_4-methane, under GIB conditions the two major products are Fe^+ and $FeSD^+$, along with minor channels leading to $FeSCD_3^+$ and $FeCD_3^+$ [138]. All species are formed in endothermic processes. DFT studies suggest that for the two competing insertion pathways, the lowest path involves a formal addition of H_3C-H across the Fe−S bond to generate a $CH_3-Fe-SH^+$ intermediate. As clearly shown in Fig. 21 [138], this bond activation step involves once more spin inversion from the sextet to the quartet surface en route to products. The occurrence of the second conceivable pathway resulting in formation of $H-Fe-SCH_3^+$ as an intermediate can be ruled out, because of the extremely high energy demands associated with overcoming the insertion barriers for either spin state of FeS^+.

4.4. Cationic metal dioxides MO_2^+: more than appetizers?

The metal dioxides MO_2^+ (M = Ti, V, Zr, Nb) in their gas-phase reactions with structurally simple substrates, e.g., water or small hydrocarbons, can be classified according to their reactivity patterns [139]. The singlet ground-state dioxides VO_2^+ and NbO_2^+ behave as closed-shell species in that no neutral radical products are produced. In contrast, the doublet-ground states for TiO_2^+ and ZrO_2^+ are better described as oxygen-centred radicals [140]. However, a closer look, augmented by extensive DFT calculations for the VO_2^+/C_2H_4 [141] and VO_2^+/C_2H_6 systems [142], reveals a Pandora's box of complexity in that, once more, two-state reactivity prevails the whole chemistry. In addition, increasing complexity is not only encountered at the electronic structure level, also reactivity patterns of a given metal dioxide can exhibit a unique dependence of product formation by slightly changing the substrate. This is clearly evidenced by the reactions of VO_2^+ with some of the most simple alkanes under ICR conditions, Fig. 22 [143].

In marked contrast to oxidative dehydrogenation followed by liberation of neutral ethene in the reaction with C_2H_6, the gas-phase chemistry of VO_2^+ with C_3H_8 mainly affords elimination of molecular hydrogen concomitant with the formation of an allyl complex (η-C_3H_5)C(O)OH^+. In the case of the next higher homologue, *n*-C_4H_{10}/VO_2^+, the combined losses of H_2 and H_2O provide yet another product channel—and preliminary calculations leave no doubt about the crucial role of several spin-inversions in the various bond activation steps [143].

5. Miscellaneous systems and outlook

Two- or multistate reactivity is also the characteristic feature of the following examples: The site-selective C−H bond activation of norbornane (*exo* versus *endo* face attack) by bare FeO^+ and the different kinetic isotope effects for activation of an *exo*- versus an *endo*-C−H bond of this substrate have been traced back to a high-spin/low-spin scenario of FeO^+ [144]. Radical-like activation of small alkanes by the ligated formal Cu^{III} oxide (phenanthroline)CuO^+ and in particular

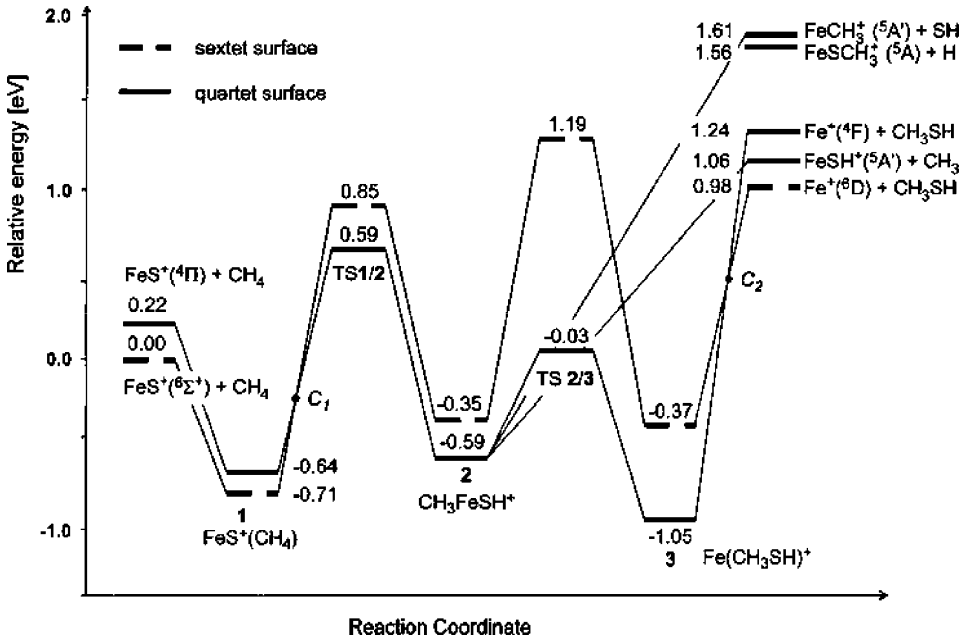

Fig. 21. B3LYP/6-311+G* potential energy curves for the FeS^+/CH_4 system. Note, that all relative energies are given in eV. C_1 and C_2 denote tentative crossing points between the sextet and quartet surfaces. Reproduced from *J. Phys. Chem. A* 105 (2001) 2005.

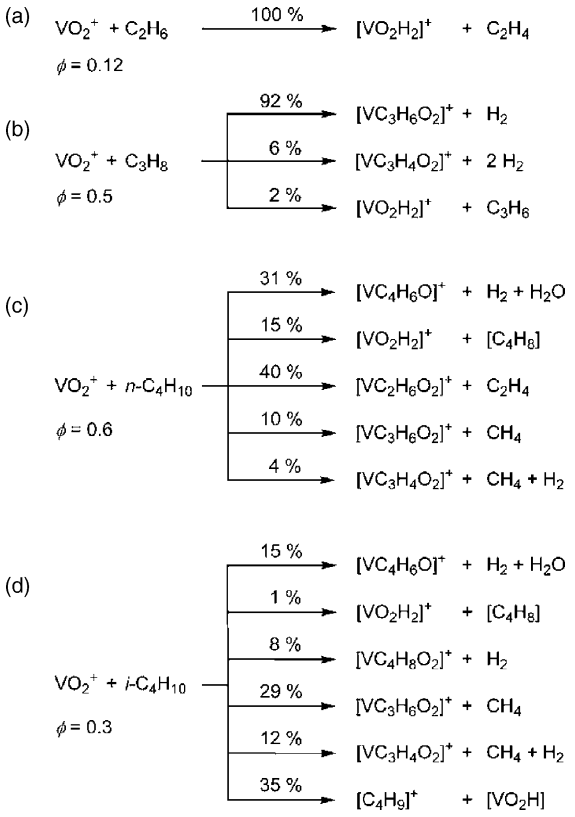

Fig. 22. Reaction efficiencies (ϕ) and primary product branching ratios for reactions of VO_2^+ with small alkanes. Reproduced from *Organometallics* 22 (2003) 3933.

the oxygenation of simple alkanes by this oxide, is also affected by a two-state reactivity pattern in the course of which the $^3A_2$ precursor metal oxide is converted to the $^1A_1$ product complex (pheanthroline)Cu^+ [145].

Similarly, the iron-mediated amination of hydrocarbons by $FeNH^+$, e.g., $CH_4 \rightarrow CH_3NH_2$, $C_6H_6 \rightarrow C_6H_5NH_2$, or $C_6H_5CH_3 \rightarrow C_6H_5CH{=}NH$, is very likely affected by the interplay of the $^6\Sigma^+$ and the $^4A'$ state of $FeNH^+$, the latter state being only 0.14 eV higher in energy than the sextet state [146].

The energetics of the interconversion of $Fe(C_2H_5)^+$ and $HFeC_2H_4^+$, a prototypical example of an organometallic β-hydrogen elimination/β-insertion process, can be lowered by a quintet → triplet → quintet hopping mechanism [147], in perfect analogy to spin-accelerated reactions as depicted in Fig. 18.

The rates, by which Mo^+ is sequentially oxidized by N_2O, Eq. (38), exhibit quite some variation for the individual oxidation steps, all of which are strongly exothermic [148a].

$$Mo^+ + N_2O \rightarrow MoO^+ + N_2 \quad (38a)$$

$k < 6 \times 10^{-13}\,cm^3\,s^{-1}\,molecule^{-1}$; $\Delta_r H^0 = -78$ kcal/mol.

$$MoO^+ + N_2O \rightarrow MoO_2{}^+ + N_2 \quad (38b)$$

$k = 5.6 \times 10^{-10}\,cm^3\,s^{-1}\,molecule^{-1}$; $\Delta_r H^0 = -87$ kcal/mol.

$$MoO_2{}^+ + N_2O \rightarrow MoO_3{}^+ + N_2 \quad (38c)$$

$k < 3.7 \times 10^{-10}\,cm^3\,s^{-1}\,molecule^{-1}$; $\Delta_r H^0 = -26$ kcal/mol.

Quite clearly, kinetic barriers must be operative in the uptake of oxygen atoms by Mo^+. For reaction (38a), an obviously inefficient crossing from sextet to the quartet state is es-

sential to make the reaction exothermic. A different situation is encountered for the next oxidation step, Eq. (38b), because formation of the quartet state of $MoO_2^+(^4A_2)$ is not too energy demanding with regard to the $MoO^+(^4\Sigma^-)$ precursor; thus, a spin-conserving reaction is feasible, and curve crossing to the low-spin dioxide $MoO_2^+(^2A_1)$ can occur at a later stage. The reaction of the latter with N_2O to $MoO_3^+(^2A_1)$ is not subject to any spin constraints and indeed takes place relatively efficiently despite having the lowest exothermicity of reactions (38a)–(38c). In an exhaustive study, Bohme and co-workers investigated the thermal reactions of 46 different atomic cations M^+ with N_2O, and the interesting periodicities observed in the oxygen-atom transfer to generate MO^+ are not only controlled by the thermochemistry of this process; rather, spin conservation is a deciding factor for the reactivity of first- and second-row metal ions while for the heavier third-row cations, as expected, spin is no longer a good quantum number [148b,148c].

The rate of CO oxidation to CO_2 by gaseous AuO^-_n (n = 1–3) exhibits features, which are controlled by both thermochemical and spin conservation aspects [149]. Triplet AuO^- ($^1\Sigma_g$) shows the highest reactivity due to a very exothermic spin-allowed oxygen atom transfer to CO. In contrast, the reaction of AuO_2^- proceeds with an extremely low rate due to a relatively high-barrier involved in the formation of the AuO_2^-(CO) encounter complex and a spin-forbidden crossing between the singlet and triplet surfaces. For AuO_3^-, the reactivity of spin-allowed CO oxidation is in-between; while the reaction is not impeded by spin-restrictions, relatively high barriers cause a decrease of the exothermic process.

Spin problems also seem to be the cause for the inertness of many transition-metal alkyl ions towards O_2. For example, while MCH_3^+ species (M = Mn, Fe, Co) are capable of activating a broad variety of organic substrates, including the inert alkanes [150], they fail to react with O_2 at appreciable rates (I. Kretzschmar, D. Schröder, H. Schwarz, unpublished results). Even the cyclopentadienyl magnesium cation $MgC_5H_5^+$ – a prototype organometallic species – remains unoxidized by O_2 in the gas phase [151], in contrast to the vigorous decomposition of metal alkyls in solution when exposed to air. In view of the favourable thermochemistry of M−C bond activation by O_2 [110], significant kinetic barriers must be operative in the gas-phase ion–molecule reactions, and the most obvious reason is failure to circumvent efficiently the spin-inversion bottleneck associated with dioxygen activation [132].

Also the activation of O_2 by atomic Cr^+, is heavily affected by a sequence of curve crossings. For example, due to spin conservation the direct formation of the doublet ground state $OCrO^+(^2A_1)$ from the ground state reactants $Cr^+(^6S)$ and $O_2(^3\Sigma_g^-)$ is not possible; rather, two curve crossings from the sextet via the quartet to the doublet surface occur in the sequence $^6Cr^+ + {}^3O_2 \rightarrow {}^6Cr(O_2)^+ \rightarrow {}^4OCrO^+ \rightarrow {}^2OCrO^+$,

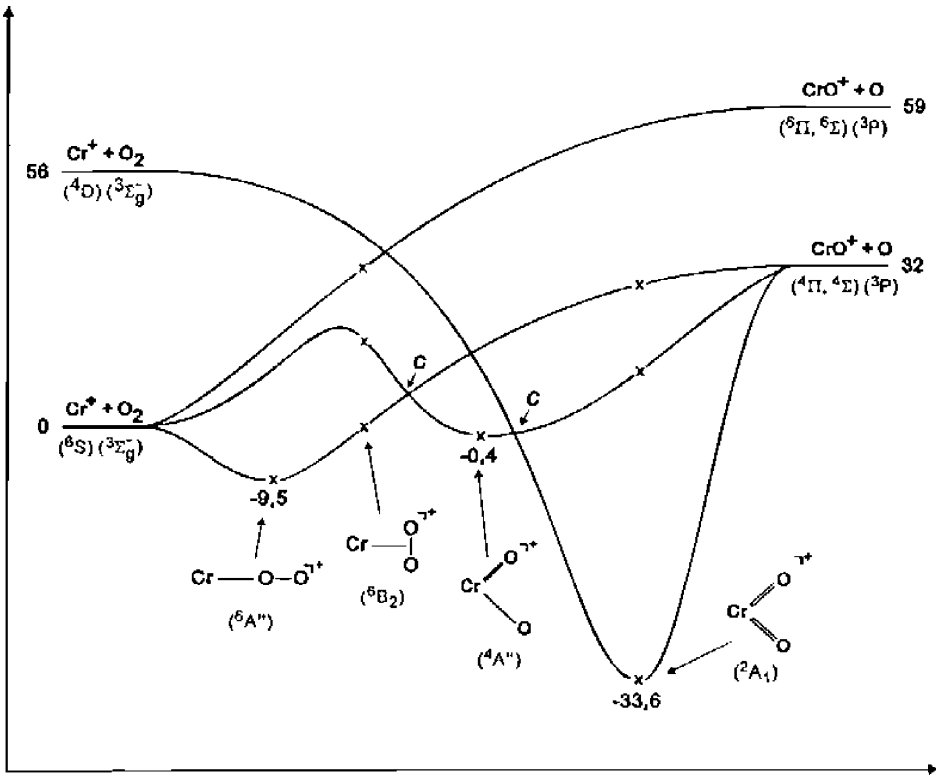

Fig. 23. Potential energy surface at the CASPT2D/BSII/LSD/DZP level of theory. Crosses denote excitation energies for the various states at the LSD geometries of the corresponding ground states. All energies are given in kcal/mol. Reproduced from *J. Am. Chem. Soc*. 118 (1996) 9941.

and the potential energy surface depicted in Fig. 23 reveals part of the complexity in this 'trivial' bond activation business of molecular oxygen [152a]. The role of a *single* water molecule acting as a catalyst in the conversion of $^6Cr(O_2)^+ \rightarrow {}^2OCrO^+$ has been studied en detail by Beyer et al. [152b].

Some of the controversies associated with the binding energies of Fe^+ to pyridine (py) and benzene (bz), derived from threshold-collision experiments of FeL^+ (L = py, bz) [153] versus competitive ligand evaporation from bisligated $Fe(bz)(py)^+$ [154] using Cooks' kinetic method [155], have been resolved in a detailed theoretical study [156]—and spin conservation aspects seem to matter a lot: starting from the bisligated ^4A complex $Fe(bz)(\sigma\text{-py})^+$, in the kinetics-method experiments in a spin-allowed dissociation the quartet states $Fe(bz)^+$ ($^4A_1$) and $Fe(\sigma\text{-py})^+$ ($^4A_1$, $^4A_2$) are produced, whose binding energies are comparable. Adiabatic formation of the much stronger bound ground state $Fe(\sigma\text{-py})^+$ ($^6A_2$), which would require a spin flip, seems to be hindered kinetically.

Various aspects, including the potential role of spin conservation/spin violation in the thermal reactions of $H_3{}^+/O$ and of small cations with atomic or molecular nitrogen were studied using selected ion flow tube mass spectrometry [157].

Among the numerous examples of small *neutral* molecules for which the gas-phase chemistry is strongly affected by spin aspects, two systems deserve to be mentioned. The notorious elusiveness of C_2O_2 (ethylene dione) [158] has found a straightforward explanation by a consideration of the potential energy curves in conjunction with the location of the minimum energy crossing point (MECP) between the singlet/triplet states of C_2O_2 and an estimate of the hopping probability to cross surfaces [158b]. The combined experimental/computational findings suggest that neutral C_2O_2 is intrinsically unstable having a maximum lifetime of ca. 0.5 ns for triplet ground state $C_2O_2(^3\Sigma_g{}^-, v = 0)$. This, for conventional mass spectrometric experiments much too short lifetime of bound $^3\Sigma_g{}^-$ C_2O_2, is essentially a consequence of the low-lying crossing point and its structural similarity to a repulsive C_2O_2 singlet state, which facilitate efficient triplet → singlet curve crossing, followed by a fast, spin-allowed dissociation to 2CO.

A classics in spin-forbidden processes is reaction (39), and in an extremely detailed theoretical study Cui et al. [159] arrived at the far-reaching conclusion by stating "it may be a poor assumption that spin-forbidden transition takes place with uniform probability on the seam of potential energy surfaces" of the mechanistically complex, multi-step bond-breaking and bond-forming reaction (39). Rather, a careful look at each minor facet seems to be essential.

$$CH(^2\Pi) + N_2 \rightarrow HCN + N(^4S) \quad (39)$$

Finally, also the thermal reactions of 'hydrated electron' clusters $(H_2O)_n{}^-$, n = 15–30, with several neutral electron scavengers, e.g., CO_2, O_2, NO exhibit reaction efficiencies the differences of which have been rationalized on the basis of spin considerations [160].

As amply demonstrated in this review, multi-state reactivity patterns are much more important than generally acknowledged and, as expressed by Harvey et al. in a related context "spin-forbidden reactions can end up being as fast as spin-allowed ones, or slower or faster! The devil is in the detail . . ." [3j]. This statement certainly holds true.

Note added in proof

In a combined experimental and theoretical study, the reactions of atomic Re^+ with H_2, HD, and D_2 have been analyzed, and the findings suggest that Re^+ reacts largely via a statistical intermediate [161]. The increased reactivity of this third-row transition metal towards dihydrogen and the stronger $M^+{-}H$ bond, in comparison to the first row congener (M=Mn) has been attributed to efficient coupling among surfaces of different spin along with lanthanide contraction and relativistic effects [161,162].

More recently, the earlier observation [162] that "bare" Zr^{2+} brings about dehydrogenation of methane (Eq. (40)) has been studied computationally [163], and it was demonstrated that this quite unusual thermal reaction is controlled by a spin change, in the course of which a triplet → singlet conversion occurs right after formation of the encounter complex $Zr(CH_4)^{2+}$ and prior to the generation of the singlet insertion intermediate $HZr(CH_3)^{2+}$.

$$^3Zr^2 + CH_4 \rightarrow {}^1ZrCH_2{}^{2+} + H_2 \quad (40)$$

A topological analysis of the gas-phase reactions of atomic $Mn^+(^7S, {}^5S)$ with H_2O, NH_3, and CH_4 has been conducted within the framework of electron localization function analysis, and the crucial part of the dehydrogenation involves a spin crossover in the course of the oxidative insertion of the metal into the X–H bond (X=HO, H_2N, H_3C) [164]. The same computational approach has been employed for studying the reactions of NH_3 with VO^+ ($^3\Sigma$, $^1\Delta$, $^5\Sigma$) and FeO^+ ($^6\Sigma$, $^4\Delta$) to produce H_2O. While for the NH_3/VO^+ couple the spin is conserved throughout the whole reaction sequence, for the FeO^+/NH_3 system several crossing points between the sextet–quartet surfaces occur on way to product formation [165].

Density functional studies have been recently reported on the mechanisms of the reactions of $OsO_n{}^+$ (n = 1−4) with methane [166]. For the systems OsO_n (n = 1, 2)/CH_4, the minimum energy reaction pathways of dehydrogenation (reaction (41)) are found to involve two spin inversions in the entrance and exit channels, respectively.

$$OsO_n{}^+(n = 1,\ 2) + CH_4 \rightarrow Os(O)_nCH_2{}^+ + H_2 \quad (41)$$

Acknowledgements

The research at TU Berlin was financially supported by generous grants from the *Deutsche Forschungsgemeinschaft*,

the *Fonds der Chemischen Industrie*, and the *BASF AG*. I am grateful for the many contributions from past and present members of my research group and for exchange of ideas with *Drs. Peter B. Armentrout, Diethard K. Bohme, Jeremy N. Harvey, Detlef Schröder, Sason Shaik* and *Kazunari Yoshizawa*. The collaboration with my long-time friend-colleague Professor Shaik and his research group at the Hebrew University of Jerusalem deserves special mentioning; joint research projects started around a decade ago and have formed the platform from which the concept of two-state reactivity eventually emerged. Technical assistance in the preparation of the article by Andrea Beck and Maria Schlangen is gratefully acknowledged.

References

[1] (a) D.R. Yarkony, Int. Rev. Phys. Chem. 11 (1992) 195;
(b) D.R. Yarkony, J. Phys. Chem. 100 (1996) 18612;
(c) S.S. Shaik, J. Am. Chem. Soc. 101 (1979) 2736;
(d) S.S. Shaik, J. Am. Chem. Soc. 101 (1979) 3184;
(e) S.S. Shaik, N.D. Epiotis, J. Am. Chem. Soc. 102 (1980) 122;
(f) M. Klessinger, J. Michl, Excited States and Photochemistry of Organic Molecules, VCH, New York, 1995.

[2] (a) P. Gütlich, Y. Garcia, H.A. Goodwin, Chem. Soc. Rev. 29 (2000) 419;
(b) P. Gütlich, Y. Garcia, T. Woike, Coord. Chem. Rev. 219 (2001) 839.

[3] (a) P.B. Armentrout, J.L. Beauchamp, Acc. Chem. Res. 22 (1989) 315;
(b) P.B. Armentrout, Annu. Rev. Phys. Chem. 41 (1990) 313;
(c) P.B. Armentrout, Science 251 (1991) 175;
(d) J.C. Weisshaar, Acc. Chem. Res. 26 (1993) 213;
(e) R. Poli, Acc. Chem. Res. 30 (1997) 494;
(f) D.A. Plattner, Angew. Chem. Int. Engl. 38 (1999) 82;
(g) D. Schröder, S. Shaik, H. Schwarz, Acc. Chem. Res. 33 (2000) 139;
(h) J.N. Harvey, in: T.R. Cundari (Ed.), Computational Organometallic Chemistry, Marcel Dekker Inc., New York, 2001, p. 291;
(i) S. Shaik, S.P. de Visser, F. Ogliaro, H. Schwarz, D. Schröder, Curr. Opin. Chem. Biol. 6 (2002) 556;
(j) J.N. Harvey, R. Poli, K.M. Smith, Coord. Chem. Rev. 238/239 (2003) 347;
(k) R. Poli, J.N. Harvey, Chem. Soc. Rev. 32 (2003) 1;
(l) F. Himo, P.E.M. Siegbahn, Chem. Rev. 103 (2003) 2421;
(m) S. Shaik, S. Cohen, S.P. de Visser, P.K. Sharma, D. Kumar, S. Kozuch, F. Ogliaro, D. Danovich, Eur. J. Inorg. Chem. (2004) 207.

[4] (a) F.C. Fehsenfeld, D.B. Dunstein, E.E. Ferguson, Planet. Space Sci. 18 (1970) 1267;
(b) F.C. Fehsenfeld, E.E. Ferguson, C.J. Howard, J. Geophys. Res. 78 (1973) 327.

[5] (a) F.C. Fehsenfeld, E.E. Ferguson, A.L. Schmeltekopf, J. Chem. Phys. 44 (1966) 3022;
(b) T.F. George, J. Ross, J. Chem. Phys. 55 (1971) 3851;
(c) J.D. Burley, K.M. Ervin, P.B. Armentrout, J. Chem. Phys. 86 (1987) 1944.

[6] (a) N. Koga, K. Morokuma, Chem. Phys. Lett. 119 (1985) 371;
(b) A. Farazdel, M. Dupuis, J. Comput. Chem. 12 (1991) 276;
(c) D.R. Yarkony, J. Phys. Chem. 97 (1993) 4407;
(d) M.J. Bearpark, M.A. Robb, H.B. Schlegel, Chem. Phys. Lett. 223 (1994) 269;
(e) J.N. Harvey, M. Aschi, H. Schwarz, W. Koch, Theor. Chem. Acc. 99 (1998) 95;
(f) D.R. Yarkony, J. Phys. Chem. A 102 (1998) 5305;
(g) J.M. Mercero, J.M. Matxain, X. Lopez, A. Largo, L.A. Eriksson, J.M. Ugalde, Int. J. Mass Spectrom., submitted for publication.

[7] (a) D.K. Bohme, in: P. Ausloos (Ed.), Interactions of Ions with Molecules, Plenum, New York, 1975;
(b) For "exceptions", see: W.E. Farneth, J.I. Brauman, J. Am. Chem. Soc. 98 (1975) 7891.

[8] K. Tanaka, L.D. Betowski, G.I. Mackay, D.K. Bohme, J. Chem. Phys. 65 (1976) 3203.

[9] A. Kasdan, E. Herbst, W.C. Lineberger, Chem. Phys. Lett. 31 (1975) 78.

[10] (a) E. Rinden, M.M. Maric, J.J. Grabowski, J. Am. Chem. Soc. 111 (1989) 1203;
(b) E.E. Ferguson, D.B. Dunkin, F.C. Fehsenfeld, J. Chem. Phys. 57 (1972) 1459;
(c) For a detailed study of various aspects of spin-forbidden deprotonation of aqueous HNO, see: V. Shafirovich, S.V. Lymar, J. Am. Chem. Soc. 125 (2003) 6547.

[11] G.A. Janaway, M. Zhong, G.G. Gatev, M.L. Chabinyc, J.I. Brauman, J. Am. Chem. Soc. 119 (1997) 11697.

[12] K. Ishiguro, M. Ozaki, N. Sekine, Y. Sawaki, J. Am. Chem. Soc. 119 (1997) 3625.

[13] J. Hu, B.T. Hill, R.R. Squires, J. Am. Chem. Soc. 119 (1997) 11699.

[14] G.F. Stowe, R.H. Schultz, C.A. Wight, P.B. Armentrout, Int. J. Mass Spectrom. Ion Process. 100 (1990) 177.

[15] M. Aschi, J.N. Harvey, C.A. Schalley, D. Schröder, H. Schwarz, Chem. Commun. (1998) 531 (and references therein).

[16] C.A. Schalley, M. Dieterle, D. Schröder, H. Schwarz, E. Uggerud, Int. J. Mass Spectrom. Ion Process. 163 (1997) 101.

[17] D.R. Yarkony, J. Am. Chem. Soc. 114 (1992) 5406.

[18] J.N. Harvey, M. Aschi, Phys. Chem. Chem. Phys. 1 (1999) 5555.

[19] J.R. Flores, C. Barrientos, A. Largo, J. Phys. Chem. 98 (1994) 1090 (and references therein).

[20] (a) M. Aschi, F. Grandinetti, J. Chem. Phys. 111 (1999) 6759;
(b) R. Sumathi, S.D. Peyerimhoff, D. Sengupta, J. Phys. Chem. A 103 (1999) 772.

[21] P.R.P. de Moraes, H.V. Linnert, M. Aschi, J.M. Riveros, J. Am. Chem. Soc. 122 (2000) 10133 (and references therein).

[22] (a) B. van de Graaf, F.W. McLafferty, J. Am. Chem. Soc. 99 (1977) 6810;
(b) W.J. Broer, W.D. Weringa, W.C. Nieuwport, Org. Mass Spectrom. 14 (1979) 543;
(c) D.W. Kuhns, T.B. Tran, S.A. Shaffer, F. Turecek, J. Phys. Chem. 98 (1994) 4845;
(d) G. Filsak, H. Budzikiewicz, J. Mass Spectrom. 34 (1999) 601.

[23] (a) E.L. Øiestad, E. Uggerud, Int. J. Mass Spectrom. Ion Process. 165 (1997) 39;
(b) E.L. Øiestad, E. Uggerud, Int. J. Mass Spectrom. Ion Process. 185 (1999) 231;
(c) D. Schröder, C.A. Schalley, N. Goldberg, J. Hrušák, H. Schwarz, Chem. Eur. J. 2 (1996) 1235;
(d) E.L. Øiestad, J.N. Harvey, E. Uggerud, J. Phys. Chem. A 104 (2000) 8382.

[24] H. Ågren, O. Vahtras, B. Minaev, Adv. Quant. Chem. 27 (1996) 71.

[25] K. Eller, H. Schwarz, Chem. Rev. 91 (1991) 1121 (and numerous references therein).

[26] (a) M. Rosi, C.W. Bauschlicher Jr., J. Chem. Phys. 90 (1989) 7264; 92 (1990) 1876;
(b) L.A. Barnes, M. Rosi, C.W. Bauschlicher Jr., J. Chem. Phys. 39 (1990) 609.

[27] R.H. Schultz, P.B. Armentrout, J. Phys. Chem. 97 (1993) 596.

[28] (a) T.F. Magnera, D.E. David, J. Michl, J. Am. Chem. Soc. 111 (1989) 4100;

(b) P.J. Marinelli, R.R. Squires, J. Am. Chem. Soc. 111 (1989) 4101;
(c) T.F. Magnera, D.E. David, D. Stulik, R.G. Orth, H.T. Jonkman, J. Michl, J. Am. Chem. Soc. 111 (1989) 5036.
[29] S.I. Gorelsky, V.V. Lavrov, G.K. Koyanagi, A.C. Hopkinson, D.K. Bohme, J. Phys. Chem. A 105 (2001) 9410.
[30] (a) T.A. Seder, A.J. Ouderdirk, E. Weitz, J. Chem. Phys. 85 (1986) 1977;
(b) For a recent, detailed computational study, which includes the location of the MECP in reaction (20), see: J.N. Harvey, M. Aschi, Faraday Discuss. 124 (2003) 129.
[31] (a) E. Weitz, J. Phys. Chem. 98 (1994) 11256;
(b) P.G. House, E. Weitz, Chem. Phys. Lett. 266 (1997) 239.
[32] (a) M.J.S. Dewar, Bull. Soc. Chem. Fr. 18 (1951) C 71;
(b) J. Chatt, L.A. Duncanson, J. Chem. Soc. (1953) 2939.
[33] P.O. Widmark, B.O. Roos, P.E.M. Siegbahn, J. Phys. Chem. 89 (1985) 2180.
[34] (a) S.R. Langhoff, C.W. Bauschlicher Jr., Annu. Rev. Phys. Chem. 39 (1988) 181;
(b) M.R.A. Blomberg, P.E.M. Siegbahn, U. Nagashima, J. Wennerberg, J. Am. Chem. Soc. 113 (1991) 424.
[35] E.A. Carter, W.A. Goddard III, J. Phys. Chem. 92 (1988) 5679.
[36] A.K. Rappé, T.H. Upton, J. Chem. Phys. 85 (1986) 4400.
[37] (a) J.L. Detrich, O.M. Reinand, A.L. Rheingold, K.H. Theopold, J. Am. Chem. Soc. 117 (1995) 11745;
(b) J.-L. Carreón-Macedo, J.N. Harvey, J. Am. Chem. Soc. 126 (2004) 5789.
[38] A.E. Alvarado-Swaisgood, J.F. Harrison, J. Phys. Chem. 89 (1985) 5198.
[39] L.M. Roth, B.S. Freiser, Mass Spectrom. Rev. 10 (1991) 303.
[40] (a) For a review on periodic trends in the reactions of no less than 44 different atomic elements A^+ with H_2, see: P.B. Armentrout, Int. Rev. Phys. Chem. 9 (1990) 115 (and references therein);
(b) J.L. Elkind, P.B. Armentrout, J. Phys. Chem. 91 (1987) 2037.
[41] B.H. Mahan, Acc. Chem. Res. 8 (1975) 55.
[42] J.L. Elkind, P.B. Armentrout, J. Phys. Chem. 89 (1985) 5626.
[43] For a comprehensive review on the electronic structures of diatomic molecules composed of 3d transition metals, see: J.F. Harrison, Chem. Rev. 100 (2000) 679 (and references therein).
[44] J.L. Elkind, P.B. Armentrout, J. Chem. Phys. 86 (1987) 1868.
[45] L.G.M. Petterson, C.W. Bauchlicher, S.R. Langhoff, H. Partridge, J. Chem. Phys. 87 (1987) 481.
[46] L. Sunderlin, N. Aristov, P.B. Armentrout, J. Am. Chem. Soc. 109 (1987) 78.
[47] (a) J.L. Elkind, P.B. Armentrout, Int. J. Mass Spectrom. Ion Process. 83 (1988) 259;
(b) J.L. Elkind, L.S. Sunderlin, P.B. Armentrout, J. Phys. Chem. 93 (1989) 3151.
[48] (a) M.A. Tolbert, J.L. Beauchamp, J. Am. Chem. Soc. 106 (1984) 8117;
(b) J.E. Bushnell, P.R. Kemper, P. Maitre, M.T. Bowers, J. Am. Chem. Soc. 116 (1994) 9710.
[49] R. Tonkyn, M. Ronan, J.C. Weisshaar, J. Phys. Chem. 92 (1988) 92.
[50] (a) M.T. Bowers, P.R. Kemper, G. von Helden, P.A.M. van Koppen, Science 260 (1993) 1446;
(b) P.R. Kemper, J. Bushnell, G. von Helden, M.T. Bowers, J. Phys. Chem. 97 (1993) 52;
(c) J.E. Bushnell, P.R. Kemper, M.T. Bowers, J. Phys. Chem. 97 (1993) 11628;
(d) J.E. Bushnell, P.R. Kemper, M.T. Bowers, J. Phys. Chem. 98 (1994) 2044.
[51] (a) C.W. Bauschlicher, S.R. Langhoff, Int. Rev. Phys. Chem. 9 (1990) 149;
(b) C.W. Bauchlicher, H. Partridge, S.R. Langhoff, J. Phys. Chem. 96 (1992) 2475;
(c) P. Maitre, C.W. Bauschlicher, J. Phys. Chem. 97 (1993) 11912;
(d) J.K. Perry, G. Ohanessian, W.A. Goddard III, J. Phys. Chem. 97 (1993) 5238.
[52] L.S. Sunderlin, P.B. Armentrout, J. Am. Chem. Soc. 111 (1989) 3845.
[53] (a) H. Schwarz, Angew. Chem. Int. Ed. Engl. 30 (1991) 820;
(b) J.M. Fox, Catal. Rev. Sci. Eng. 35 (1993) 169;
(c) R.H. Crabtree, Chem. Rev. 95 (1995) 987;
(d) G.A. Olah, A. Molnar, Hydrocarbon Chemistry, Wiley, New York, 1995;
(e) B.A. Arndtsen, R.G. Bergman, T.A. Mobley, T.H. Petersen, Acc. Chem. Res. 28 (1995) 154;
(f) J.H. Lunsford, Catal. Today 63 (2000) 165;
(g) H. Arakawa, M. Aresta, J.N. Armor, M.A. Barteau, E.J. Beckman, A.T. Bell, J.E. Bercaw, C. Creutz, E. Dinjus, D.A. Dixon, K. Doman, D.L. DuBois, J. Eckert, E. Fujita, D.H. Gibson, W.A. Goddard, D.W. Goodman, J. Keller, G.J. Kubas, H.H. Kung, J.E. Lyons, L.E. Manzer, T.J. Marks, K. Morokuma, K.M. Nicholas, R. Periana, L. Que, J. Rostrup-Nielson, W.M.H. Sachtler, L.D. Schmidt, A. Sen, G.A. Somorjai, P.C. Stair, B.R. Stults, W. Tumas, Chem. Rev. 101 (2001) 953;
(h) R.H. Crabtree, J. Chem. Soc. Dalton Trans. (2001) 1551;
(i) J.A. Labinger, J.E. Bercaw, Nature 417 (2002) 1551;
(j) A.A. Fokin, P.R. Schreiner, Chem. Rev. 102 (2002) 1551;
(k) R.A. Periana, O. Mironov, H. Taube, G. Bhalla, C.J. Jones, Science 301 (2003) 814.
[54] Chem. Eng. News 71 (1993) 27.
[55] (a) D. Schröder, H. Schwarz, Angew. Chem. Int. Ed. Engl. 29 (1990) 1433;
(b) H. Schwarz, D. Schröder, Pure Appl. Chem. 72 (2000) 2319 (and references therein).
[56] (a) L.F. Halle, P.B. Armentrout, J.L. Beauchamp, J. Am. Chem. Soc. 103 (1981) 962;
(b) R. Georgiadis, P.B. Armentrout, J. Phys. Chem. 92 (1988) 7067.
[57] (a) M.P. Irion, A. Selinger, Ber. Bunsenges. Phys. Chem. 93 (1989) 1408;
(b) S.W. Buckner, T.J. MacMahon, G.D. Byrd, B.S. Freiser, Inorg. Chem. 28 (1989) 3511;
(c) J.K. Perry, G. Ohanessian, W.A. Goddard III, Organometallics 13 (1994) 1870;
(d) P.B. Armentrout, M.R. Sievers, J. Phys. Chem. A 107 (2003) 4396 (and references therein).
[58] C.J. Carpenter, P.A.M. von Koppen, M.T. Bowers, J.K. Perry, J. Am. Chem. Soc. 122 (2000) 392 (and references therein).
[59] (a) G. Albert, C. Berg, M. Beyer, U. Achatz, S. Joos, G. Niedner-Schatteburg, V.E. Bondybey, Chem. Phys. Lett. 268 (1997) 235;
(b) K. Koszinowski, M. Schlangen, D. Schröder, H. Schwarz, submitted for publication.
[60] (a) C. Hinderling, D.A. Plattner, P. Chen, Angew. Chem. Int. Ed. Engl. 36 (1997) 243;
(b) C. Hinderling, D. Feichtinger, D.A. Plattner, P. Chen, J. Am. Chem. Soc. 119 (1997) 10793.
[61] (a) K.K. Irikura, J.L. Beauchamp, J. Am. Chem. Soc. 111 (1989) 75;
(b) K.K. Irikura, J.L. Beauchamp, J. Am. Chem. Soc. 113 (1991) 2769;
(c) K.K. Irikura, J.L. Beauchamp, J. Phys. Chem. 95 (1991) 8344.
[62] (a) D.G. Musaev, K. Morokuma, Isr. J. Chem. 33 (1993) 307;
(b) D.G. Musaev, N. Koga, K. Morokuma, J. Phys. Chem. 97 (1993) 4064;
(c) D.G. Musaev, K. Morokuma, N. Koga, K.A. Nguyen, M.S. Gordon, R. Cundari, J. Phys. Chem. 97 (1993) 11435;
(d) M.R.A. Blomberg, P.E.M. Siegbahn, M. Svensson, J. Phys. Chem. 98 (1994) 2062;
(e) C. Heinemann, R. Hertwig, R. Wesendrup, W. Koch, H. Schwarz, J. Am. Chem. Soc. 117 (1995) 495;
(f) J.J. Caroll, J.C. Weisshaar, P.E.M. Siegbahn, C.A.M. Wittborn, M.R.A. Blomberg, J. Phys. Chem. 99 (1995) 14388;

(g) C. Heinemann, H. Schwarz, W. Koch, K.G. Dyall, J. Chem. Phys. 104 (1996) 4642;
(h) D.G. Musaev, K. Morokuma, J. Phys. Chem. 100 (1996) 11600;
(i) M. Hendrickx, M. Ceulemans, L. Vanquickenborne, Chem. Phys. Lett. 257 (1996) 8;
(j) M. Pavlov, M.R.A. Blomberg, P.E.M. Siegbahn, R. Wesendrup, C. Heinemann, H. Schwarz, J. Phys. Chem. A 101 (1997) 1567;
(k) U. Achatz, M. Beyer, S. Joos, B.S. Fox, G. Niedner-Schtteburg, V.E. Bondybey, J. Phys. Chem. A 103 (1999) 8200;
(l) For a recent review on the role of relativistic effects in gas-phase ion chemistry, see: H. Schwarz, Angew. Chem. Int. Ed. 42 (2003) 4442 (and references therein).

[63] (a) A. Kaldor, D.M. Cox, Pure Appl. Chem. 62 (1990) 79;
(b) U. Achatz, C. Berg, S. Joos, B.S. Fox, M.K. Beyer, G. Niedner-Schatteburg, V.E. Bondybey, Chem. Phys. Lett. 320 (2000) 53;
(c) K. Koszinowski, D. Schröder, H. Schwarz, J. Phys. Chem. A 107 (2003) 4999;
(d) K. Koszinowski, D. Schröder, H. Schwarz, Chem. Phys. Chem. 4 (2003) 121;
(e) K. Koszinowski, D. Schröder, H. Schwarz, J. Am. Chem. Soc. 125 (2003) 121;
(f) K. Koszinowski, D. Schröder, H. Schwarz, Angew. Chem. Int. Ed. 43 (2004) 121;
(g) K. Koszinowski, D. Schröder, H. Schwarz, Organometallics 23 (2004) 1132.

[64] (a) N. Aristov, P.B. Armentrout, J. Phys. Chem. 91 (1987) 6178;
(b) L.S. Sunderlin, P.B. Armentrout, J. Phys. Chem. 92 (1988) 1209;
(c) R.H. Schultz, J.L. Elkind, P.B. Armentrout, J. Am. Chem. Soc. 110 (1988) 411;
(d) R. Georgiadis, P.B. Armentrout, J. Phys. Chem. 92 (1988) 7060.

[65] S. Chiodo, O. Kondakova, M. del Carmen Michelini, N. Russo, E. Sicilia, A. Irigoras, J.M. Ugalde, J. Phys. Chem. A 108 (2004) 1069 (and reference therein).

[66] D.G. Musaev, K. Morokuma, J. Chem. Phys. 101 (1994) 10697.

[67] R.H. Schultz, P.B. Armentrout, J. Phys. Chem. 97 (1993) 596.

[68] M. Hendrickx, K. Gong, L. Vanquickenborne, J. Chem. Phys. 107 (1997) 6299.

[69] R.H. Schultz, P.B. Armentrout, J. Phys. Chem. 91 (1987) 4433.

[70] N. Russo, E. Sicilia, J. Am. Chem. Soc. 123 (2001) 2588.

[71] B.L. Kickel, P.B. Armentrout, J. Am. Chem. Soc. 117 (1995) 4057.

[72] B.L. Kickel, P.B. Armentrout, J. Am. Chem. Soc. 116 (1994) 10742.

[73] B.L. Kickel, P.B. Armentrout, J. Am. Chem. Soc. 117 (1995) 764.

[74] B.L. Kickel, E.R. Fisher, P.B. Armentrout, J. Phys. Chem. 96 (1992) 2603.

[75] T.R. Cundari, M.S. Gordon, J. Phys. Chem. 96 (1992) 631.

[76] (a) L. Sanders, S.D. Hanton, J.C. Weisshaar, J. Chem. Phys. 92 (1990) 3498;
(b) L. Sanders, S.D. Hanton, J.C. Weisshaar, J. Chem. Phys. 92 (1990) 3485.

[77] P.A.M. van Koppen, M.T. Bowers, C.L. Haynes, P.B. Armentrout, J. Am. Chem. Soc. 120 (1998) 5704.

[78] E.R. Fisher, P.B. Armentrout, J. Am. Chem. Soc. 114 (1992) 2049.

[79] (a) N. Aristov, P.B. Armentrout, J. Am. Chem. Soc. 108 (1986) 1806;
(b) L. Sanders, S. Hanton, J.C. Weisshaar, J. Phys. Chem. 91 (1987) 5145.

[80] J.L. Beauchamp, ACS Symp. Ser. 333 (1987) 11.

[81] J.B. Schilling, J.L. Beauchamp, J. Am. Chem. Soc. 110 (1988) 15.

[82] (a) M.C. Holthausen, A. Fiedler, H. Schwarz, W. Koch, Angew. Chem. Int. Ed. Engl. 34 (1995) 2282;
(b) M.C. Holthausen, W. Koch, Helv. Chim. Acta 79 (1996) 1939.

[83] (a) B. Schilling, J.L. Beauchamp, Organometallics 7 (1988) 194;
(b) R. Georgiadis, P.B. Armentrout, Int. J. Mass Spectrom. Ion Process. 89 (1989) 227.

[84] (a) W.D. Reents, F. Strobel, R.B. Freas, J. Wronka, D.P. Ridge, J. Phys. Chem. 89 (1985) 5666;
(b) J.L. Elkind, P.B. Armentrout, J. Chem. Phys. 86 (1987) 1868.

[85] M. Rosi, C.W. Bauschlicher, S.R. Langhoff, H. Partridge, J. Phys. Chem. 94 (1990) 8656.

[86] (a) S.W. Buckner, J.R. Gord, B.S. Freiser, J. Am. Chem. Soc. 110 (1988) 6606;
(b) D.E. Clemmer, P.B. Armentrout, J. Phys. Chem. 95 (1991) 3090.

[87] D.E. Clemmer, L.S. Sunderlin, P.B. Armentrout, J. Phys. Chem. 94 (1990) 3008.

[88] B.C. Guo, K.P. Gerns, A.W. Castleman Jr., J. Phys. Chem. 96 (1992) 4879.

[89] Y. Nakao, T. Taketsugu, K. Hirao, J. Chem. Phys. 110 (1999) 10863.

[90] (a) A. Mavridis, F.L. Herrera, J.F. Harrison, J. Phys. Chem. 95 (1991) 6854;
(b) S. Kapellos, A. Mavridis, J.F. Harrison, J. Phys. Chem. 95 (1991) 6860.

[91] D. Walter, P.B. Armentrout, J. Am. Chem. Soc. 120 (1998) 3176.

[92] (a) Y.-M. Chen, D.E. Clemmer, P.B. Armentrout, J. Phys. Chem. 98 (1994) 11490;
(b) D.E. Clemmer, Y.-M. Chen, P.B. Armentrout, J. Phys. Chem. 98 (1994) 7538.

[93] J.L. Tilson, J.F. Harrison, J. Phys. Chem. 95 (1991) 5097.

[94] A. Irigoras, J.E. Fowler, J.M. Ugalde, J. Am. Chem. Soc. 121 (1999) 574.

[95] A. Irigoras, J.E. Fowler, J.M. Ugalde, J. Phys. Chem. A 102 (1998) 293.

[96] D.E. Clemmer, Y.-M. Chen, F.A. Khan, P.B. Armentrout, J. Phys. Chem. 98 (1994) 6522.

[97] A. Irigoras, J.E. Fowler, J.M. Ugalde, J. Am. Chem. Soc. 121 (1999) 8549.

[98] A. Irigoras, O. Elizalde, I. Silanes, J.E. Fowler, J.M. Ugalde, J. Am. Chem. Soc. 122 (2000) 114.

[99] C. Rue, P.B. Armentrout, I. Kretzschmar, D. Schröder, J.N. Harvey, H. Schwarz, J. Chem. Phys. 110 (1999) 7858.

[100] M.R. Sievers, P.B. Armentrout, J. Chem. Phys. 102 (1995) 754.

[101] I. Kretzschmar, D. Schröder, H. Schwarz, C. Rue, P.B. Armentrout, J. Phys. Chem. A 102 (1998) 10060.

[102] C. Rue, P.B. Armentrout, I. Kretzschmar, D. Schröder, H. Schwarz, Int. J. Mass Spectrom. 210/211 (2001) 283.

[103] (a) C. Rue, P.B. Armentrout, I. Kretzschmar, D. Schröder, H. Schwarz, J. Phys. Chem. A 105 (2001) 8456;
(b) I. Kretzschmar, D. Schröder, H. Schwarz, C. Rue, P.B. Armentrout, J. Phys. Chem. A 104 (2000) 5046;
(c) C. Rue, P.B. Armentrout, I. Kretzschmar, D. Schröder, H. Schwarz, J. Phys. Chem. A 106 (2002) 9788.

[104] T. Baer, W.L. Hase, Unimolecular Reaction Dynamics, Oxford University Press, New York, 1996.

[105] G.E. Zahr, R.K. Preston, W.H. Miller, J. Chem. Phys. 62 (1975) 1127.

[106] (a) E.I. Stiefel, K. Matsumoto (Eds.), Transition Metal Sulfur Chemistry, ACS Symposium Series, vol. 653, Washington, 1996;
(b) V.E. Heinrich, P.A. Cox, The Surface Science of Metal Oxides, Cambridge University Press, Oxford, 1994.

[107] R.H. Holm, P. Kennepohl, E.I. Solomon, Chem. Rev. 96 (1996) 2239.

[108] (a) E. Drobner, H. Huber, G. Wächtershäuser, K.O. Stetter, Nature 346 (1990) 742;
(b) G. Wächtershäuser, in: E.-L. Winnacker (Ed.), Unter jedem Stein liegt ein Diamant: Struktur–Dynamik–Evolution, S. Hirzel Verlag, Stuttgart, 2001, p. 15.

[109] I. Kretzschmar, D. Schröder, H. Schwarz, P.B. Armentrout, Adv. Metal Semiconductor Clusters 5 (2001) 347.

[110] D. Schröder, H. Schwarz, S. Shaik, Struct. Bonding 97 (2000) 91.

[111] E.A. Carter, W.A. Goddard, J. Phys. Chem. 92 (1988) 2109.

[112] D. Schröder, H. Schwarz, Angew. Chem. Int. Ed. Engl. 34 (1995) 1973.
[113] M.F. Ryan, A. Fiedler, D. Schröder, H. Schwarz, J. Am. Chem. Soc. 117 (1995) 2033.
[114] H. Kang, J.L. Beauchamp, J. Am. Chem. Soc. 108 (1986) 7502.
[115] A.E. Stevens, J.L. Beauchamp, J. Am. Chem. Soc. 101 (1979) 6449.
[116] T.C. Jackson, D.B. Jacobson, B.S. Freiser, J. Am. Chem. Soc. 106 (1984) 1252.
[117] D.E. Clemmer, N.F. Dalleska, P.B. Armentrout, Chem. Phys. Lett. 190 (1992) 259.
[118] T.C. Jackson, T.J. Carlin, B.S. Freiser, J. Am. Chem. Soc. 108 (1986) 1120.
[119] D.E. Clemmer, N. Aritsov, P.B. Armentrout, J. Phys. Chem. 97 (1993) 544.
[120] A. Fiedler, D. Schröder, S. Shaik, H. Schwarz, J. Am. Chem. Soc. 116 (1994) 10734.
[121] D. Schröder, A. Fiedler, M.F. Ryan, H. Schwarz, J. Phys. Chem. 98 (1994) 68.
[122] S. Shaik, D. Danovich, A. Fiedler, D. Schröder, H. Schwarz, Helv. Chim. Acta 78 (1995) 1393.
[123] V. Baranov, G. Javahery, A.C. Hopkinson, D.K. Bohme, J. Am. Chem. Soc. 117 (1995) 12801.
[124] D. Schröder, H. Schwarz, D.E. Clemmer, Y. Chen, P.B. Armentrout, V.I. Baranov, D.K. Bohme, Int. J. Mass Spectrom. Ion Process. 161 (1997) 175.
[125] D. Danovich, S. Shaik, J. Am. Chem. Soc. 119 (1997) 1773.
[126] M. Filatov, S. Shaik, J. Phys. Chem. A 102 (1998) 3835.
[127] (a) A. Fiedler, J. Hrušák, H. Schwarz, Z. Phys. Chem. 175 (1992) 15;
(b) A. Fiedler, J. Hrušák, W. Koch, H. Schwarz, Chem. Phys. Lett. 211 (1993) 242.
[128] (a) S. Shaik, M. Filatov, D. Schröder, H. Schwarz, Chem. Eur. J. 4 (1998) 193;
(b) N. Harris, S. Cohen, M. Filatov, F. Ogliaro, S. Shaik, Angew. Chem. Int. Ed. Engl. 39 (2000) 2003;
(c) F. Ogliaro, N. Harris, S. Cohen, M. Filatov, S.P. de Visser, S. Shaik, J. Am. Chem. Soc. 122 (2000) 8977.
[129] I. Schlichting, J. Berendzen, K. Chu, A.M. Stock, S.A. Maves, D.E. Benson, R.M. Sweet, D. Ringe, G.A. Petsko, S.G. Seigar, Science 287 (2000) 1615.
[130] D.H.R. Barton, Aldrichim. Acta 23 (1990) 3.
[131] A.J. Bard, G.M. Whitesides, R.N. Zare, F.W. McLafferty, Acc. Chem. Res. 28 (1995).
[132] D. Schröder, H. Schwarz, in: G. Quinkert, M.V. Kisakürek (Eds.), Essays in Contemporary Chemistry: From Molecular Structure Towards Biology, Verlag Helvetica Chimica Acta, Zürich, 2001, p. 131.
[133] (a) S.S. Stahl, S.J. Lippard, in: G.C. Ferreira, J.J.G. Moura, R. Franco (Eds.), Dioxygen and Alkane Activation by Iron-Containing Enzymes, Wiley-VCH, Weinheim, 1999, p. 303;
(b) G.C. Ferreira, J.J.G. Moura, R. Franco, Iron Metabolism: Inorganic Biochemistry and Regulatory Mechanisms, Wiley-VCH, Weinheim, 1999;
(c) B. Meunier, Metal-Oxo and Metal-Peroxo Species in Catalytic Oxidations, Springer, Berlin, 2000;
(d) P.E.M. Siegbahn, M.R.A. Blomberg, Chem. Rev. 100 (2000) 421.
[134] (a) K. Yoshizawa, Y. Shiota, T. Yamabe, Chem. Eur. J. 3 (1997) 1160;
(b) K. Yoshizawa, Y. Shiota, T. Yamabe, J. Am. Chem. Soc. 120 (1998) 564;
(c) K. Yoshizawa, Y. Shiota, T. Yamabe, J. Chem. Phys. 111 (1999) 538;
(d) Y. Shiota, K. Yoshizawa, J. Am. Chem. Soc. 122 (2000) 12317;
(e) Y. Shiota, K. Yoshizawa, J. Chem. Phys. 118 (2003) 5872.
[135] T. Su, J. Chem. Phys. 88 (1988) 3102;
T. Su, J. Chem. Phys. 89 (1988) 5355.
[136] K. Koszinowski, D. Schröder, H. Schwarz, Eur. J. Inorg. Chem. (2004) 44 (and references therein).
[137] S. Bärsch, I. Kretzschmar, D. Schröder, H. Schwarz, P.B. Armentrout, J. Phys. Chem. A 103 (1999) 5925.
[138] S. Bärsch, D. Schröder, H. Schwarz, P.B. Armentrout, J. Phys. Chem. A 105 (2001) 2005.
[139] J.N. Harvey, M. Diefenbach, D. Schröder, H. Schwarz, Int. J. Mass Spectrom. 182/183 (1999) 85.
[140] For an excellent discussion on this classification scheme, as well as other aspects of metal-assisted oxygenation reactions, see: C. Limberg, Angew. Chem. Int. Ed. 42 (2003) 5932 (and references therein).
[141] L. Gracia, J.R. Sambrano, V.S. Safont, M. Calatayad, A. Beltrán, J. Andrés, J. Phys. Chem. A 107 (2003) 3107.
[142] L. Gracia, J. Andrés, V.S. Safont, A. Beltrán, J.R. Sambrano, Organometallics 23 (2004) 730.
[143] M. Engeser, M. Schlangen, D. Schröder, H. Schwarz, T. Yumura, K. Yoshizawa, Organometallics 19 (2003) 3933.
[144] N. Harris, S. Shaik, D. Schröder, H. Schwarz, Helv. Chim. Acta 82 (1999) 1784.
[145] D. Schröder, M.C. Holthausen, H. Schwarz, J. Phys. Chem. A 108 (2004).
[146] M. Brönstrup, I. Kretzschmar, D. Schröder, H. Schwarz, Helv. Chim. Acta 81 (1998) 2348.
[147] A. Fiedler, D. Schröder, W. Zummack, H. Schwarz, Inorg. Chim. Acta 259 (1997) 227.
[148] (a) I. Kretzschmar, A. Fiedler, J.N. Harvey, D. Schröder, H. Schwarz, J. Phys. Chem. A 101 (1997) 6252;
(b) V.V. Lavrov, V. Blagojevic, G.K. Koyanagi, G. Orlova, D.K. Böhme, J. Phys. Chem. A 108 (2004);
(c) Also see: A.J. Lorquet, J.C. Lorquet, W. Forst, J. Chem. Phys. 51 (1980) 253.
[149] M.L. Kimble, A.W. Castleman Jr., R. Mitric, L. Bürgel, V. Bonačic-Koutecky, J. Am. Chem. Soc. 126 (2004) 2526.
[150] B. Jacobsen, J.R. Good, B.S. Freiser, Organometallics 8 (1989) 2957 (and references therein).
[151] R.K. Milburn, V. Baranov, A.C. Hopkinson, D.K. Bohme, J. Phys. Chem. A 103 (1999) 6373.
[152] (a) A. Fiedler, I. Kretzschmar, D. Schröder, H. Schwarz, J. Am. Chem. Soc. 118 (1996) 9941;
(b) M.K. Beyer, C.B. Berg, U. Achatz, S. Joos, G. Niedner-Schatteburg, V.E. Bondybey, Mol. Phys. 99 (2001) 699.
[153] (a) F. Meyer, F.A. Khan, P.B. Armentrout, J. Am. Chem. Soc. 117 (1995) 9740;
(b) M.T. Rodgers, J.R. Stanley, R. Amminnugana, J. Am. Chem. Soc. 122 (2000) 10969;
(c) M.T. Rodgers, P.B. Armentrout, Mass Spectrom. Rev. 19 (2000) 215 (and references therein).
[154] (a) D. Schröder, H. Schwarz, J. Organomet. Chem. 504 (1995) 123;
(b) S. Ma, P. Wong, S.S. Yang, R.G. Cooks, J. Am. Chem. Soc. 118 (1996) 6010.
[155] (a) R.G. Cooks, T.L. Krüger, J. Am. Chem. Soc. 99 (1977) 1279;
(b) R.G. Cooks, P.S.H. Wong, Acc. Chem. Res. 31 (1998) 379.
[156] M. Diefenbach, C. Trage, H. Schwarz, Helv. Chim. Acta 86 (2003) 1008 (and references therein).
[157] (a) D.B. Milligan, M.J. McEwan, Chem. Phys. Lett. 319 (2000) 482;
(b) G.B.I. Scott, D.A. Fairley, C.G. Freeman, M.J. McEwan, V.G. Anicich, J. Chem. Phys. 109 (1998) 9010.
[158] (a) G. Maier, M. Naumann, H.P. Reisenauer, J. Eckwert, Angew. Chem. Int. Ed. Engl. 35 (1996) 1696;
(b) D. Schröder, C. Heinemann, H. Schwarz, J.N. Harvey, S. Dua, S.J. Blanksby, J.H. Bowie, Chem. Eur. J. 4 (1998) 2550.

[159] Q. Cui, K. Morokuma, J.M. Bowman, S.J. Klippenstein, J. Chem. Phys. 110 (1999) 9469.
[160] S.T. Arnold, R.A. Morris, A.A. Viggiano, M.A. Johnson, J. Phys. Chem. 100 (1996) 2900.
[161] P.B. Armentrout, F.-X. Li, J. Chem. Phys. 121 (2004) 248.
[162] Y.A. Ranasinghe, T.J. McMahon, B.S. Freiser, J. Phys. Chem. 95 (1991) 7721.
[163] M. Kaczorowska, J.N. Harvey, in preparation.
[164] (a) M. Carmen Michelini, N. Russo, E. Sicilia, J. Phys. Chem. A 106 (2002) 8937;
(b) M. Carmen Michelini, E. Sicilia, N. Russo, M.E. Alikhaus, B. Silvi, J. Phys. Chem. A 107 (2003) 4862.
[165] S. Chiodo, O. Kondakova, M. Carmen Michelini, N. Russo, E. Sicilia, Inorg. Chem. 42 (2003) 8773.
[166] G. Zhang, S. Li, Y. Jiang, Organometallics 23 (2004) 3656.